

Currency Network Risk*

Mykola Babiak**

Lancaster University Management School

Jozef Baruník***

Charles University

Abstract

This paper identifies a new currency risk stemming from linkages between option-implied currency volatilities. A volatility network strategy that buys net recipients and sells net transmitters of transitory shocks to ex-ante currency volatilities generates significant excess returns. Net recipients are more exposed to volatility spillovers and compensate investors with higher average returns. In contrast, net transmitters are more resilient to volatility transmissions and offer a lower risk premium because they hedge against volatility interdependencies. When volatility linkages are controlled for contemporaneous correlations, the strategy is uncorrelated with popular benchmarks. The volatility network factor is also priced in a currency cross-section.

Keywords: Currency predictability, network risk, currency volatility, option-implied volatility, persistence, term structure

JEL: G12, G15, F31

*We appreciate the valuable discussions of Saleem Bahaj (discussant), Mete Kilic (discussant), Guofu Zhou (discussant), and the helpful comments of Vikas Agarwal, Kevin Aretz, Mattia Bevilacqua, Daniele Bianchi, Pasquale Della Corte, Michael Ellington, Massimo Guidolin, Amit Goyal, Roman Kozhan, Ingmar Nolte, Grzegorz Pawlina, Bryan Routledge, Mark Shackleton, Ivan Shaliastovich, Radu Tunaru, and conference participants at the 2023 Western Finance Association (WFA) Meeting, the 2023 Conference of Swiss Society for Financial Market Research (SGF), the 2023 European Economic Association (EEA) Meeting, the 2022 European Finance Association (EFA) Meeting, the 2022 International Symposium on Forecasting (ISF), the 2022 Slovak Economic Association Meeting (SEAM), and 3rd Annual Bristol Financial Markets Conference.

**Lancaster University Management School, Bailrigg, LA1 4YX, Lancaster, UK, E-mail: m.babiak@lancaster.ac.uk.

***Institute of Economic Studies, Charles University, Opletalova 26, 110 00, Prague, CR and Institute of Information Theory and Automation, Academy of Sciences of the Czech Republic, Pod Vodarenskou Vezi 4, 18200, Prague, Czech Republic, E-mail: barunik@utia.cas.cz.

1 Introduction

Volatility has played a central role in economics and finance. In currency markets, a global volatility risk has been proposed by prior literature as a key driver of carry trade returns (Lustig, Roussanov, and Verdelhan, 2011; Menkhoff, Sarno, Schmeling, and Schrimpf, 2012a). While the global volatility risk factor is intuitively appealing, there is little evidence on how individual currency volatilities relate to each other. This seems surprising since a shock to the ex-ante volatility of a particular currency possibly transmits to expectations about the future volatility of other currencies. These linkages consequently define weighted and directed network structures that contain information about the transmission of volatility shocks among individual currencies above and beyond fluctuations in global volatility. Since the connections are likely to be asymmetric, investors are unable to diversify away from idiosyncratic shocks and hence differences in the strength of directional volatility connections become important characteristics of currency risk. Guided by this insight and earlier evidence on network effects for firm-level stock volatilities (Herskovic, Kelly, Lustig, and Van Nieuwerburgh, 2020), our goal is to understand currency volatility linkages and to test whether currency excess returns compensate for such risk.

In this paper, we identify time-varying linkages among option-based currency volatilities that possess heterogeneous degrees of persistence originating from transitory and persistent components of volatility shocks. Using traded currency options, we measure how market expectations about future exchange rate fluctuations covary across currencies and how shocks to these expectations create a network and spread within that network.¹ The pure market-based approach we propose allows us to characterize the currency volatility network risk on a daily basis as well as to use its forward-looking strength at the cost of minimal assumptions. We document two important sources of risk stemming from volatility linkages. Currencies that are more exposed to volatility shocks from others compensate investors for being vulnerable and earn a higher risk premium. In contrast, currencies that transmit more volatility shocks to others than receive offer a lower risk premium because

¹Surprisingly, the literature on the information content of currency options is limited compared to the evidence on equity options. Notable exceptions making use of dollar options include Campa and Chang (1995), Della Corte, Ramadorai, and Sarno (2016), Londono and Zhou (2017), and Della Corte, Kozhan, and Neuberger (2021), whereas Jurek (2014), Mueller, Stathopoulos, and Vedolin (2017), and Della Corte, Kozhan, and Neuberger (2022) employ cross currency options.

they hedge against volatility spillovers. Exploring the time variation in volatility networks, we show that the information contained in asymmetric volatility connections is valuable for an investor.

The main contribution of the paper is that we present new empirical evidence regarding the behavior of option-based currency volatilities and examine the implications of this behavior for exchange rate predictability. First, ex-ante volatilities of currencies form a connected network. The network connections are driven by a strong correlation component. Second, a network strategy that buys net recipients and sells net transmitters of transitory linkages between currency volatilities generates a significant Sharpe ratio. When volatility linkages are controlled for contemporaneous correlations, the portfolio formed on such asymmetric connections is uncorrelated with popular benchmarks and generates a significant alpha. The network risk factor is also priced in a currency cross-section. Third, we identify network structures with a heterogeneous degree of persistence stemming from transitory and persistent components of shocks that create various types of risk for investors. We document a downward-sloping term structure of network risk.

We begin our empirical investigation by constructing forward-looking measures of exchange rate volatilities from currency option prices, following the model-free approach of [Britten-Jones and Neuberger \(2000\)](#) and [Bakshi, Kapadia, and Madan \(2003\)](#).^{2,3} We continue by constructing a novel forward-looking dynamic network of option-implied volatilities on exchange rates. Our network measures are built in the tradition of dynamic predictive modeling under misspecification, and linkages are approximated via time-varying parameter vector autoregression models ([Diebold and Yilmaz, 2014](#); [Barunik and Ellington, 2020](#)). Specifically, the network of individual volatilities inferred from time-varying variance decompositions and its frequency domain counterpart has several key attributes. First, the connections between the volatilities are weighted and directed. That is, the influence of shocks to exchange rate volatilities is not symmetric in the system and such a

²The highly liquid and large foreign exchange volatility market provides an excellent opportunity to synthesize such measures. As of June 2019, the daily average turnover was \$294 billion and notional amounts outstanding was \$12.7 trillion ([BIS, 2019a,b](#)). A wide variety of strikes and maturities available on the market allow us to precisely compute the option-implied variances on exchange rates.

³The variance measures constructed from currency derivatives, which reflect the expectations of agents about future financial and real macroeconomic risks, are distinct from the backward-looking realized variance estimates. See, for example, [Gabaix and Maggiori \(2015\)](#), [Zviadadze \(2017\)](#), and [Colacito, Croce, Gavazzoni, and Ready \(2018\)](#) for the nature of risks traded in currency markets.

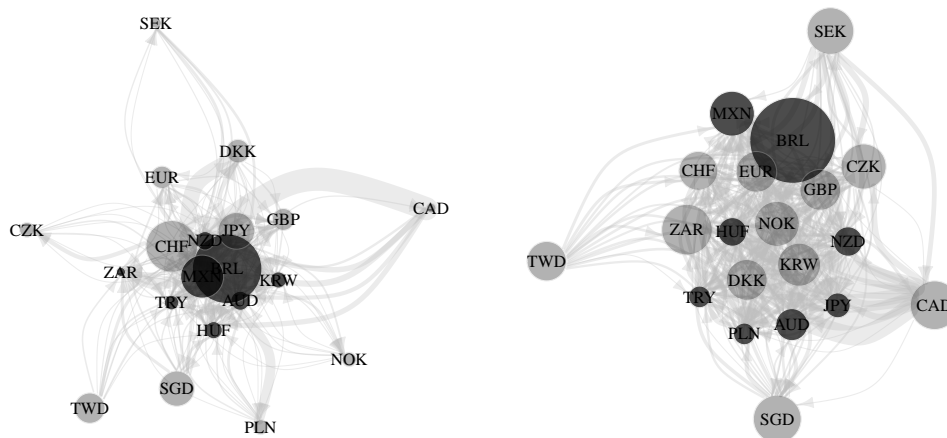


Figure 1. Transitory (left) and persistent (right) volatility networks: September 30, 2008

The left (right) figure depicts a transitory (persistent) network among option-implied currency volatilities based on connections of the transitory (permanent) nature of shocks. We remove the contemporaneous effects in volatility linkages by diagonalizing the covariance matrix. Arrows denote the direction of connections and the strength of lines denotes the strength of linkages. Grey (black) vertices denote currencies receiving (transmitting) more shocks than transmitting (receiving). The size of vertices indicates the net amount of shocks. To enhance the readability, links are drawn if intensities are above a predetermined threshold.

network then identifies information beyond standard correlation-based measures. Second, we are able to distinguish connections among individual currency volatilities with heterogeneous persistence. Thus, we shed light on how a network risk stemming from shocks with different persistence is being priced in currency markets. Third, international dependencies are naturally driven by common fluctuations in global markets. In our analysis, we examine the networks based on the asymmetric impact of shocks after controlling for contemporaneous variation in individual volatilities. Our network measures allow characterizing such dependencies by isolating linkages among currency volatilities controlled for contemporaneous effects. Finally, the structure of volatility connections is changing dynamically over time, unlike the somewhat persistent relationships between countries based on interest rates. Hence, sorting currencies according to volatility linkages is not equivalent, for example, to the currency carry trade.

To illustrate the above, Figure 1 depicts the network structures among currency volatilities of twenty developed and emerging market economies inferred from shocks of (i) transitory (short-term) nature of up to one week and (ii) persistent (long-term) nature of longer than one month shortly after the bankruptcy of Lehman Brothers, following severely con-

tracted liquidity at the end of September 2008. It is worth emphasizing that even after controlling for contemporaneous correlation in the global markets, the volatility network contains rich information about volatility shocks having both transitory and persistent impacts. A natural question arises: what are the asset pricing implications of the network structures capturing currency volatility linkages beyond contemporaneous correlations?

We document that such network structures predict currency returns. Empirically, we examine the profitability of strategies that buy net recipients and sell net transmitters of volatility shocks. For each currency volatility, we first compute the cumulative strength of transmitted/received shocks with a given persistence level and take the difference between them to obtain a net-directional connectedness at a given horizon. We consider three degrees of shock persistence with short-, medium-, and long-term horizons.⁴ We then build monthly quintile portfolios sorted by the net-directional network measures. For instance, for the short-term net-directional network, the first (fifth) portfolio contains the currencies transmitting (receiving) more short-term shocks than receiving (transmitting) them. We find that buying currencies of short-term net recipients and selling currencies of short-term net transmitters yields a Sharpe ratio of 0.60 over the 1996-2023 period.⁵ Regressing the excess returns of short-term net-directional portfolios on the dollar, carry trade, volatility, volatility risk premium, and momentum strategies yields economically and statistically significant alphas (5.01% per annum with a t-stat of 3.25). To better understand the sources of this profitability, we sort the currencies into quintiles based on a combined strength of all transmitted (received) shocks to (from) others. The results show that this is the network risk related to transmitting shocks to others, which has a strong predictive power.

Relative to common currency risk factors, the predictability stemming from network risk is primarily driven by changes in exchange rates and not by interest rate differentials. Furthermore, the network strategies are weakly and even negatively correlated with currency benchmarks, providing excellent diversification gains. Intuitively, the network strategy is formed on shock transitions not driven by a common correlation in volatilities. Since the latter is an important component of standard currency portfolios, especially the

⁴In the empirical investigation, we define short-term as a 1-day to 1-week horizon, medium-term as a 1-week to 1-month horizon, and long-term as a horizon longer than 1-month.

⁵For comparison, currency carry trade and momentum produce Sharpe ratios of 0.48 and 0.31 during the same period, whereas a volatility risk premium portfolio earns lower risk-adjusted returns. The weak performance of standard strategies is primarily driven by strong underperformance after the Financial Crisis.

carry trade, the profitability of the network strategy cannot be understood using traditional risk factors. The allocation analysis demonstrates that the strategy using short-term net-directional connections buys or sells different currencies compared to benchmarks around 40% of the time. The results indicate a distinctive source of network returns.

We next focus on the term structure of network risk premiums. The risk-adjusted performance of network portfolios formed on net-directional connectedness decreases with the persistence of volatility linkages, suggesting that excess returns are related to transitory shocks. This complements the evidence of the downward-sloping term structure of unconditional variance risk premium in equity markets (Dew-Becker, Giglio, Le, and Rodriguez, 2017). Interestingly, average returns and Sharpe ratios of strategies formed on the number of transmitted shocks slightly increase with the horizon.

Further, we examine whether excess returns of network-sorted portfolios reflect the compensation for risk. For this purpose, we consider the cross-section of currency returns formed on the transitory net-directional connectedness. Following Lustig, Roussanov, and Verdelhan (2011), we perform a principal component decomposition of test portfolios. Motivated by these results, we formally test a battery of two- and three-factor linear models. We document that none of the pricing kernels with benchmark factors can explain currency network returns. Meanwhile, the network factor appears to be strongly priced.

We perform a number of additional checks. First, the magnitude and significance of returns of network portfolios increase when we move to a weekly frequency. Second, the excess returns remain significant after adjusting them for transaction costs. Third, the network portfolios generate comparable performance statistics before and after the Global Financial Crisis, in contrast to benchmark strategies whose performance significantly deteriorates in the second sub-sample. Fourth, our results work equally well for network risk measures estimated from option-implied variances instead of volatilities. Finally, the predictive power of volatility network risk disappears when estimated from realized currency volatilities, highlighting the importance of forward-looking option-based volatilities.

This paper contributes to the literature documenting predictability in currency returns.⁶

⁶The literature proposes strategies, among others, based on the carry trade (Lustig and Verdelhan, 2007; Lustig, Roussanov, and Verdelhan, 2011; Menkhoff, Sarno, Schmeling, and Schrimpf, 2012a), momentum (Menkhoff, Sarno, Schmeling, and Schrimpf, 2012b; Asness, Moskowitz, and Pedersen, 2013; Dahlquist and

The volatility-related strategies exploit global foreign exchange volatility ([Menkhoff, Sarno, Schmeling, and Schrimpf, 2012a](#)) and currency volatility risk premium ([Della Corte, Ramadorai, and Sarno, 2016](#); [Londono and Zhou, 2017](#)). [Gabaix and Maggiori \(2015\)](#) and [Colacito, Croce, Gavazzoni, and Ready \(2018\)](#) build the models explaining these strategies. We contribute to this literature by showing how network risk from option-based volatilities on exchange rates is priced in the cross-section of currency excess returns. Further, network returns are virtually unrelated to the existing strategies. [Della Corte, Kozhan, and Neuberger \(2021\)](#) document a global risk factor in the cross-section of implied volatility returns. The key differentiator of our study from their work is that we propose volatility network risk and study its predictive power for spot currency returns.

In related work, [Mueller, Stathopoulos, and Vedolin \(2017\)](#) propose a strategy based on the sensitivity of currencies to the cross-sectional dispersion of conditional foreign exchange correlation. They construct the conditional correlation from spot exchange rates as well as using the currency options for the risk-neutral counterpart. They find some interesting results about the compensation for exposure to high or low dispersion states. In contrast, we focus on dependencies in option-based volatilities. The connectedness measures of our paper are directional, unlike symmetric correlation-based proxies.

Our paper is also related to [Richmond \(2019\)](#) who presents a model explaining the carry trade premium via the country's position in the global trade network. Unlike network risk based on trade linkages, we study the market-based network from option-based volatilities. The predictability of currency excess returns sorted on network risk measures primarily stems from changes in exchange rates and not interest rate differentials. Hence, the predictive information of the network factor built is distinctive from trade links.

Finally, our paper is related to the literature on downside risk in currency markets. [Jurek \(2014\)](#), [Burnside, Eichenbaum, Kleshchelski, and Rebelo \(2011\)](#), [Farhi, Fraiberger, Gabaix, Ranciere, and Verdelhan \(2015\)](#) and [Chernov, Graveline, and Zviadadze \(2018\)](#) investigate currency crash risk, while [Fan, Londono, and Xiao \(2021\)](#) document an option-based equity tail factor in currency returns. Although we use currency options data, our paper examines the dependencies among currency volatilities instead of downside risk.

[Hasseltoft, 2020](#)), business cycles ([Colacito, Riddiough, and Sarno, 2020](#)), and global imbalances ([Corte, Riddiough, and Sarno, 2016](#)).

2 Currency Network Risk

This section describes the construction of option-implied currency variances, outlines the procedure used to estimate network connections between individual volatilities, and then introduces currency network risk proxies studied in the core analysis.⁷

2.1 Currency Volatility: Inferring Investor's Expectations from Option Prices

We begin by synthesizing the risk-neutral expectation of exchange rate variances from quoted currency options. We obtain spot implied variances from OTC currency options by applying a model-free approach of Britten-Jones and Neuberger (2000) and Bakshi, Kapadia, and Madan (2003). Formalizing the discussion, we use prices of European call and put options expiring at time $t + \tau$ to compute the annualized risk-neutral expectation of the return variance of an exchange rate k versus the US dollar between t and $t + \tau$:

$$E_t^Q \left[(RV_{t,\tau}^k)^2 \right] = \frac{2}{B^k(t, t + \tau)} \left\{ \int_{F^k(t, t + \tau)}^{\infty} \frac{C^k(t, t + \tau, K)}{K^2} dK + \int_0^{F^k(t, t + \tau)} \frac{P^k(t, t + \tau, K)}{K^2} dK \right\}, \quad (1)$$

where $RV_{t,\tau}^k$ is the realized volatility of the underlying asset, $E_t^Q[\cdot]$ denotes the expectation operator under the risk-neutral probability measure Q , $C^k(t, t + \tau, K)$ and $P^k(t, t + \tau, K)$ denote the prices of call and put contracts at time t with a strike price K and maturity τ , $B^k(t, t + \tau)$ is the price of a country's bond at time t with maturity τ , $F^k(t, t + \tau)$ is the forward exchange rate of the currency k at time t with maturity τ . To compute the model-free implied variances, we discretize the integral in Eq. (1) by adopting call and put option prices interpolated around the τ maturity, and by considering a range of strike prices for the currency k .

Two comments are noteworthy at this point. First, large swings in currency volatilities will produce even larger fluctuations in variances due to convexity, especially during periods of crises. This may artificially imply a stronger connectedness. Following the definition of the volatility risk premium strategy (Della Corte, Ramadorai, and Sarno, 2016) and the forward volatility contract (Della Corte, Kozhan, and Neuberger, 2021) in currency markets, our empirical analysis examines the linkages between implied volatilities

⁷Appendix A provides a detailed methodology used to estimate a dynamic horizon-specific network.

$\sqrt{E_t^Q [(RV_{t,\tau}^k)^2]}$.⁸ Second, the important characteristic of the network risk among individual currency volatilities is the forward-looking nature of risk-neutral variances synthesized from currency derivatives. It is intuitively obvious that their predictive nature should be distinct from backward-looking realized variances. In robustness checks, we demonstrate that indeed the predictive power of network structures in realized volatilities almost completely disappears. Our results emphasize the importance of using the information content of currency options data.

2.2 *Dynamic Network Risk*

Having constructed forward-looking expectations of currency volatilities, our objective is to define the network for shocks of a specific persistence propagating across these volatilities. The knowledge of how an uncertainty shock to a currency j transmits to a currency k defines a directed link at a given period of time. These disaggregate connections between currency pairs then characterize two major types of network risk: a recipient or a transmitter of volatility shocks. Aggregating the information from all pairs provides a system-wide measure of the forward-looking connectedness among foreign exchange rates of countries.

A dynamic network can be characterized well through variance decompositions from a time-varying parameter vector autoregression (TVP-VAR) approximation model (Diebold and Yilmaz, 2014). Variance decompositions provide useful information about how much of the future variance of a variable j is due to shocks in a variable k . The time-varying variance decomposition matrix defines a dynamic network adjacency matrix, which is retrieved over different frequencies of interest.⁹ Unlike classical network structures with binary, symmetric, and static connections, the horizon-specific dynamic adjacency matrices in our analysis allow for weighted and directed connections, creating asymmetries in various measures summarising the properties of the network. These measures are the key to our analysis as directional connectedness risk stems directly from asymmetries within the network.

⁸In robustness checks, we demonstrate that our results remain unchanged if we use implied variances. We choose to work with volatilities for a better comparison with the existing literature.

⁹A natural way to characterize horizon-specific dynamics (e.g., short- and long-term) of the dynamic network risk is to consider the spectral representation of the approximating model as recently proposed by Barunik and Ellington (2020).

We construct a dynamic network through the TVP-VAR model estimated from currency implied volatilities following the methodology of [Barunik and Ellington \(2020\)](#). We consider a locally stationary TVP-VAR of a lag order p describing the dynamics as:

$$\mathbf{CIV}_{t,T} = \Phi_1(t/T)\mathbf{CIV}_{t-1,T} + \dots + \Phi_p(t/T)\mathbf{CIV}_{t-p,T} + \epsilon_{t,T}, \quad (2)$$

where $\mathbf{CIV}_{t,T} = \left(\mathbf{CIV}_{t,T}^{(1)}, \dots, \mathbf{CIV}_{t,T}^{(N)} \right)^\top$ is a double indexed N -variate time series of currency volatilities, $\epsilon_{t,T} = \Sigma^{-1/2}(t/T)\boldsymbol{\eta}_{t,T}, \boldsymbol{\eta}_{t,T} \sim NID(0, \mathbf{I}_M)$ are normally distributed shocks,

$$\Phi(t/T) = (\Phi_1(t/T), \dots, \Phi_p(t/T))^\top$$

are the time-varying autoregressive coefficients. Note that t refers to a discrete-time index $1 \leq t \leq T$ and T is an additional index indicating the sharpness of the local approximation of the time series by a stationary process. Rescaling time such that the continuous parameter $u \approx t/T$ is a local approximation of the weakly stationary time-series ([Dahlhaus, 1996](#)), we approximate $\mathbf{CIV}_{t,T}$ in a neighborhood of $u_0 = t_0/T$ by a stationary process:

$$\widetilde{\mathbf{CIV}}_t(u_0) = \Phi_1(u_0)\widetilde{\mathbf{CIV}}_{t-1}(u_0) + \dots + \Phi_p(u_0)\widetilde{\mathbf{CIV}}_{t-p}(u_0) + \epsilon_t. \quad (3)$$

The TVP-VAR process has a time-varying Vector Moving Average $VMA(\infty)$ representation ([Dahlhaus, Polonik, et al., 2009](#); [Barunik and Ellington, 2020](#)):

$$\mathbf{CIV}_{t,T} = \sum_{h=-\infty}^{\infty} \Psi_{t,T}(h)\epsilon_{t-h} \quad (4)$$

where a parameter vector $\Psi_{t,T}(h) \approx \Psi(t/T, h)$ is a time-varying impulse response function characterized by a bounded stochastic process.¹⁰ Information contained in $\Psi_{t,T}(h)$ permits the measurement of the contribution of shocks in the system. Hence, its transformations over time will determine the network risk. Since a shock to a variable in the model does not necessarily appear alone, an identification scheme is crucial in identifying the network. We adapt the extension of the generalized identification scheme of [Pesaran and Shin \(1998\)](#) to locally stationary process as proposed by [Barunik and Ellington \(2020\)](#).

¹⁰Since $\Psi_{t,T}(h)$ contains an infinite number of lags, we approximate the moving average coefficients at $h = 1, \dots, H$ horizons.

We transform local impulse responses in the system into local impulse transfer functions using Fourier transformations. This allows us to measure the horizon-specific dynamics of the network based on the heterogeneous persistence of shocks in the system. A dynamic representation of the variance decomposition of shocks from a currency j 's volatility to a currency k 's volatility then establishes a dynamic horizon-specific adjacency matrix, which is central to our network risk measures.

Specifically, the element of such a matrix, which captures a portion of the local error variance of the volatility of a currency j is due to shocks in the volatility of a currency k at a given point of time $u = t_0/T$ and a given horizon $d_i \in \mathcal{H} = \{S, M, L\}$, is formally defined as:

$$\left[\boldsymbol{\theta}(u, d_i)\right]_{j,k} = \frac{\hat{\sigma}_{kk}^{-1} \sum_{\omega \in d_i} \left(\left[\hat{\Psi}(u, \omega) \hat{\Sigma}(u) \right]_{j,k} \right)^2}{\sum_{\omega \in \mathcal{H}} \left[\hat{\Psi}(u, \omega) \hat{\Sigma}(u) \hat{\Psi}^\top(u, \omega) \right]_{j,j}}. \quad (5)$$

$\hat{\Psi}(u, \omega) = \sum_{h=0}^{H-1} \sum_h \hat{\Psi}(u, h) e^{-i\omega h}$ is an impulse transfer function estimated from Fourier frequencies ω of impulse responses that cover a specific horizon d_i , which is one of short (S), medium (M), or long (L) horizons as defined for arbitrarily chosen bands of frequencies.¹¹ It is important to note that $\left[\boldsymbol{\theta}(u, d)\right]_{j,k}$ is a natural disaggregation of traditional variance decompositions to a time-varying and h -horizon adjacency matrix. This is because the portion of the local error variance of the j -th variable at horizon h due to shocks in the k -th variable is scaled by the total variance of the j -th variable. As the rows of the dynamic adjacency matrix do not necessarily sum to one, we normalize the element in each by the corresponding row sum:

$$\left[\tilde{\boldsymbol{\theta}}(u, d)\right]_{j,k} = \left[\boldsymbol{\theta}(u, d)\right]_{j,k} / \sum_{k=1}^N \left[\boldsymbol{\theta}(u, d)\right]_{j,k} \quad (6)$$

Eq. (6) defines a dynamic horizon-specific network completely. Naturally, our adjacency matrix is filled with weighted links showing the strengths of connections. The links are directional, meaning that the j to k link is not necessarily the same as the k to j link. In sum, the adjacency matrix is horizon-specific, asymmetric, and evolves dynamically.

¹¹Note that $i = \sqrt{-1}$.

To obtain the time-varying coefficient estimates $\hat{\Phi}_1(u), \dots, \hat{\Phi}_p(u)$ and the time-varying covariance matrix $\hat{\Sigma}(u)$ at a given point of time $u = t_0/T$, we estimate the approximating model in Eq. (3) using Quasi-Bayesian Local-Likelihood (QBLL) methods (Petrova, 2019). Specifically, we use a kernel weighting function, which gives larger weights to those observations surrounding the period whose coefficient and covariance matrices are of interest. Using conjugate priors, the (quasi) posterior distribution of the parameters of the model is available analytically. This alleviates the need to use a Markov Chain Monte Carlo (MCMC) simulation algorithm and permits the use of parallel computing. We provide a detailed discussion of the estimation algorithm in Appendix A. We also publish the computationally efficient packages `DynamicNets.jl` in JULIA and `DynamicNets` in MATLAB that can be used to replicate our network connectedness measures.¹²

2.3 Network Risk Measures

The elements of the adjacency matrix displayed in Table 1 completely specify the horizon-specific network connections in each period of time. We define the network connectedness measure as the ratio of the off-diagonal elements to the sum of the entire matrix:

$$\mathcal{C}(u, d) = \frac{\sum_{\substack{j,k=1 \\ k \neq j}}^N [\tilde{\theta}(u, d)]_{j,k}}{\sum_{j,k=1}^N [\tilde{\theta}(u, d)]_{j,k}} \quad d \in \{S, M, L\}. \quad (7)$$

This quantifies the contribution of forecast error variance due to all shocks in the system, excluding the contribution of own shocks. The network connectedness measure is computed for the connections with a pre-specified persistence, which can be one of three choices: short- (S), medium- (M), or long-run (L). These horizons are determined by chosen bands of frequencies and aim to cover transitory, less persistent, and more persistent shocks. The sum of these measures across all frequency bands defines the combined network connectedness $\mathcal{C}(u, T) = \sum_{d \in \{S, M, L\}} \mathcal{C}(u, d)$ at time u .

We also define disaggregate network connectedness measures that reveal when an individual currency volatility is a stronger transmitter or recipient of shocks. The from-directional connectedness measures how much of each currency's j volatility is due to

¹²The packages are available at <https://github.com/barunik/DynamicNets.jl> and <https://github.com/mte00/DynamicNets>.

Table 1. Dynamic Adjacency Matrix

This table presents a time-varying adjacency matrix for volatility shock propagation. The element $[\tilde{\theta}(u, d)]_{j,k}$ of such a matrix captures a portion of the local error variance of the volatility of a currency j due to shocks in the volatility of a currency k at a given point of time u and a given horizon $d \in \{S, M, L\}$. The from-directional connectedness of a currency j is the sum of elements in the row j excluding the one on the main diagonal. The to-directional connectedness of a currency j is the sum of elements in the column j excluding the one on the main diagonal.

Currency	1	2	...	N	$\mathcal{F}_{j \leftarrow \bullet}(u, d)$
1	$[\tilde{\theta}(u, d)]_{1,1}$	$[\tilde{\theta}(u, d)]_{1,2}$...	$[\tilde{\theta}(u, d)]_{1,N}$	$\sum_{k \neq 1} [\tilde{\theta}(u, d)]_{1,k}$
2	$[\tilde{\theta}(u, d)]_{2,1}$	$[\tilde{\theta}(u, d)]_{2,2}$...	$[\tilde{\theta}(u, d)]_{2,N}$	$\sum_{k \neq 2} [\tilde{\theta}(u, d)]_{2,k}$
\vdots	\vdots	\vdots	\ddots	\vdots	\vdots
N	$[\tilde{\theta}(u, d)]_{N,1}$	$[\tilde{\theta}(u, d)]_{N,2}$...	$[\tilde{\theta}(u, d)]_{N,N}$	$\sum_{k \neq N} [\tilde{\theta}(u, d)]_{N,k}$
$\mathcal{T}_{j \rightarrow \bullet}(u, d)$	$\sum_{k \neq 1} [\tilde{\theta}(u, d)]_{k,1}$	$\sum_{k \neq 2} [\tilde{\theta}(u, d)]_{k,2}$...	$\sum_{k \neq N} [\tilde{\theta}(u, d)]_{k,N}$	

shocks of other currencies' volatilities $j \neq k$ in the cross-section and is given by:

$$\mathcal{F}_{j \leftarrow \bullet}(u, d) = \sum_{\substack{k=1 \\ k \neq j}}^N [\tilde{\theta}(u, d)]_{j,k} \quad d \in \{S, M, L\}. \quad (8)$$

Likewise, the to-directional connectedness measures the contribution of each currency's j volatility to the volatilities of other currencies and is given by:

$$\mathcal{T}_{j \rightarrow \bullet}(u, d) = \sum_{\substack{k=1 \\ k \neq j}}^N [\tilde{\theta}(u, d)]_{k,j} \quad d \in \{S, M, L\}. \quad (9)$$

One can interpret these measures as dynamic to-degrees and from-degrees that associate with the nodes of the weighted directed network captured by a variance decomposition matrix. The two measures show how other currencies contribute to the risk of a currency j , and how a currency j contributes to the riskiness of others in a time-varying fashion at a horizon d . Adding these measures across all horizons defines a combined impact $\mathcal{F}_{j \leftarrow \bullet}(u, T) = \sum_{d \in \{S, M, L\}} \mathcal{F}_{j \leftarrow \bullet}(u, d)$ and $\mathcal{T}_{j \rightarrow \bullet}(u, T) = \sum_{d \in \{S, M, L\}} \mathcal{T}_{j \rightarrow \bullet}(u, d)$. We define a horizon-specific net-directional connectedness measure as:

$$\mathcal{N}_{j \rightarrow \bullet}(u, d) = \mathcal{T}_{j \rightarrow \bullet}(u, d) - \mathcal{F}_{j \leftarrow \bullet}(u, d) \quad d \in \mathcal{H} = \{S, M, L, T\}. \quad (10)$$

Naturally, if the net-directional network measure is positive (negative) for a currency, then we can interpret this currency as a net transmitter (net recipient) of shocks in the network. The main aim of this paper is to study the asset pricing implications of from-, to-, and net-directional network risks defined by Eq. (8)-(10) in a currency cross-section.

3 Data and Currency Portfolios

3.1 Currency Options Data

We start our empirical investigation by collecting daily OTC option implied volatilities on exchange rates versus the US dollar from JP Morgan and Bloomberg. Following [Della Corte, Ramadorai, and Sarno \(2016\)](#) and [Della Corte, Kozhan, and Neuberger \(2021\)](#), we consider a sample of the following 20 developed and emerging market countries: Australia, Brazil, Canada, the Czech Republic, Denmark, Euro Area, Hungary, Japan, Mexico, New Zealand, Norway, Poland, Singapore, South Africa, South Korea, Sweden, Switzerland, Taiwan, Turkey, and the United Kingdom. The data cover the sample period from January 1996 to January 2023. The cross-section begins with 10 currencies and gradually increases over time, with the data on all exchange rates being available from 2004 until the end of the sample in 2023.¹³

We synthesize spot implied variances using a model-free approach of [Britten-Jones and Neuberger \(2000\)](#), which requires currency option prices for a range of strike prices. Quotes for OTC currency options are expressed in terms of [Garman and Kohlhagen \(1983\)](#) implied volatilities for selected combinations of plain-vanilla options (at-the-money, 10 and 25 delta put and call options). We recover strike prices from deltas and option prices from implied volatilities by employing interest rates from Bloomberg, and spot and forward exchange rates from Barclays and Reuters via Datastream. Using this recovery procedure, we obtain plain vanilla European calls and puts for exchange rates versus the US dollar for a range of maturities: 1 month, 3 months, 6 months, 12 months, and 24 months.

Since our investment strategy is carried out at the monthly frequency, it is natural to assume that traders prefer to employ the 1-month implied volatilities on exchange rates for detecting network risk instead of using data for longer maturities. We, therefore, work

¹³We greatly appreciate the help of Roman Kozhan with the currency options data.

with the 1-month volatilities in our empirical analysis. Further, we estimate the network using the volatilities at the daily frequency to increase the number of observations in our estimation procedure and ultimately to better capture the dynamic nature of network risk. We then filter end-of-month estimates of how currencies are connected to each other to construct the long-short network portfolios.

3.2 Exchange Rate Data

We retrieve daily bid, mid, and ask spot and forward exchange rates versus the US dollar from Barclays and Reuters via Datastream. We further obtain daily nominal interest rates for domestic (the US in our case) and foreign countries from Bloomberg. The core empirical analysis is conducted at the monthly frequency and hence we sample end-of-month observations of all time series. We match exchange and interest rate data with currency options data for the cross-section of 20 countries and the sample period from January 1996 to January 2023 as described above.

3.3 Currency Excess Returns

We denote the spot and forward exchange rates of foreign currency k at time t as S_t^k and F_t^k . Exchange rates are expressed in units of foreign currency per US dollar. Thus, an increase in S_t^k indicates a depreciation of the foreign currency. Following [Menkhoff, Sarno, Schmeling, and Schrimpf \(2012a\)](#), we define one-period ahead excess return to a US investor for holding foreign currency k at time t as

$$rx_{t+1}^k = i_t^k - i_t - \Delta s_{t+1}^k \approx f_t^k - s_{t+1}^k, \quad (11)$$

in which i_t^k and i_t represent the risk-less rates of the foreign country k and the US, Δs_{t+1}^k is the log change in the spot exchange rate, f_t^k and s_{t+1}^k denote the log spot and forward rates. Under covered interest rate parity (CIP), the interest rate differential $i_t^k - i_t$ is equal to a forward discount $f_t^k - s_t^k$. Thus, the approximation in Eq. (11) states that the currency excess return equals the difference between the current forward rate and the future spot rate. The early literature documented that CIP held even for very short horizons ([Akram, Rime, and Sarno, 2008](#)), while recent evidence has shown CIP deviations in the post-global financial crisis period ([Du, Tepper, and Verdelhan, 2018](#); [Andersen, Duffie, and Song, 2019](#)).

We demonstrate that the profitability of network strategies studied in our paper stems primarily from spot exchange rate predictability. Therefore, our key results do not depend on the validity of the CIP condition.

3.4 Network Portfolios

The network measures introduced in Section 2.3 capture multiple risks that could be important for investors forming currency portfolios. First, unlike the previous literature focusing on the correlation risk in currency returns, the network risk proxies of our paper can identify the nature of linkages by removing contemporaneous effects. Thus, we are able to detect novel risks originating from the propagation of shocks in the network of exchange rate volatilities beyond common correlations. Second, using individual connections between exchange rates, we can quantify the aggregate amount of shocks that a particular currency transmits to or receives from others. Similarly, we can compute the net-directional connectedness measure by taking the difference between shocks that are transmitted and received. Third, a large strand of the literature studies the role of shocks with different persistence. For instance, long-term fluctuations in expected growth and volatility of cash-flows (Bansal and Yaron, 2004) have played a central role in understanding equity, bond, and currency returns. Our econometric methodology allows us to disentangle the effect of horizon-specific linkages. We can therefore shed light on the term structure of network risk. In sum, we construct a battery of portfolios based on a variety of network measures to quantitatively evaluate which network risks are priced in currency markets.

At the end of each time period t (the last day of the month), we sort currencies into five portfolios using one of the network measures constructed and described in Section 2.3. The first quintile portfolio \mathcal{P}_1 comprises 20% of all currencies with the highest values of a particular network characteristic, whereas the fifth quintile portfolio \mathcal{P}_5 contains 20% of all currencies with the lowest values. Each \mathcal{P}_i is an equally weighted portfolio of the corresponding currencies. We next form a long-short strategy that buys \mathcal{P}_5 and sells \mathcal{P}_1 .

We report the results for five quintile portfolios and a long-short strategy sorted by (i) short- (S), medium- (M), and long-term (L) as well as total (T) net-directional connectedness. The corresponding zero-cost strategies are denoted by $\mathcal{N}(d)$ in which $d \in \{S, M, L, T\}$. We additionally dissect the sources of profitability of net-directional network

strategies by solely looking at the risk of being a stronger transmitter or a stronger recipient of shocks. In particular, we construct the portfolios based on (ii) to-directional and (iii) from-directional connectedness measures. Similarly to the portfolios in (i), we report the results for all horizons considered. The respective to-directional and from-directional long-short portfolios are denoted by $\mathcal{T}(d)$ and $\mathcal{F}(d)$ in which $d \in \{S, M, L, T\}$.

3.5 Dollar and Carry Trade Strategies

We compare the performance of network-sorted portfolios to standard strategies from the existing literature. Following [Lustig, Roussanov, and Verdelhan \(2011\)](#), we build a portfolio that is the average of all currencies available in a particular time period. The resulting returns are equivalent to borrowing money in the US and investing in global money markets outside the US. This strategy is commonly called the dollar risk factor or the dollar portfolio (dol). Further, we sort all currencies available at time t into five quintile on the basis of their interest rate differential (or forward premia) relative to the US. The first quintile portfolio \mathcal{P}_1 comprises 20% of all currencies with the highest interest rates, whereas the fifth quintile portfolio \mathcal{P}_5 contains 20% of all currencies with the lowest interest rates. The difference between \mathcal{P}_1 and \mathcal{P}_5 is called the carry trade strategy (car), which is equivalent to borrowing money in low interest rate countries and investing in high interest rate countries.

3.6 Volatility Portfolios

We create a strategy taking into account past realized volatility of currencies in the spirit of [Menkhoff, Sarno, Schmeling, and Schrimpf \(2012a\)](#). At the end of each month t , we compute the square root of the sum of squared daily log exchange rate returns during the current month. We sort all currencies available at time t into five quintile portfolios on the basis of their monthly realized volatility. The first quintile portfolio \mathcal{P}_1 comprises 20% of all currencies with the highest volatility, whereas the fifth quintile portfolio \mathcal{P}_5 contains 20% of all currencies with the lowest volatility. The difference between \mathcal{P}_1 and \mathcal{P}_5 is called the volatility strategy (vol), which is equivalent to selling currencies of low volatility risk countries and buying those of high volatility risk countries.

3.7 Volatility Risk Premium Portfolios

We construct a strategy reflecting the costs of insuring currency volatility risk recently proposed by [Della Corte, Ramadorai, and Sarno \(2016\)](#). At the end of each month t , we compute the volatility risk premium (vrp) for each currency defined as the difference between expected realized volatility and implied volatility over the next month.¹⁴ We sort all currencies available at time t into five quintile portfolios on the basis of their monthly vrp. The first quintile portfolio \mathcal{P}_1 comprises 20% of all currencies with the highest vrp, whereas the fifth quintile portfolio \mathcal{P}_5 contains 20% of all currencies with the lowest vrp. The difference between \mathcal{P}_1 and \mathcal{P}_5 is called the volatility risk premia strategy, which is equivalent to selling high-insurance-cost currencies and buying low-insurance-cost currencies.

3.8 Momentum Portfolios

We form a tradable strategy linked to the past performance of currencies as initially proposed by [Menkhoff, Sarno, Schmeling, and Schrimpf \(2012b\)](#). Recently, [Dahlquist and Hasseltoft \(2020\)](#) connect currency returns to past trends in fundamentals including economic activity and inflation. Following [Dahlquist and Hasseltoft \(2020\)](#), at the end of each month t , we compute the average of currency excess returns over the last twelve months.¹⁵ We sort all currencies available at time t into five quintile portfolios on the basis of their trend. The first quintile portfolio \mathcal{P}_1 comprises 20% of all currencies with the highest average returns, whereas the fifth quintile portfolio \mathcal{P}_5 contains 20% of all currencies with the lowest average returns. The difference between \mathcal{P}_1 and \mathcal{P}_5 is called the momentum strategy (mom), which is equivalent to selling past losers (or worst-performing currencies) and buying past winners (or best-performing currencies).

4 Network Risk and Currency Returns

4.1 Network Connectedness Dynamics and Contemporaneous Correlations

We now estimate the network connectedness in option-based currency volatilities driven by shocks of various degrees of persistence (transitory, less persistent, and more persistent).

¹⁴[Della Corte, Ramadorai, and Sarno \(2016\)](#) work with the one-year volatility risk premium. We decide to switch to the monthly horizon to ensure that the volatility risk premium strategy employs one-month implied volatilities on exchange rates consistent with network portfolios.

¹⁵Our results remain quantitatively similar for other lags over which the past performance is evaluated.

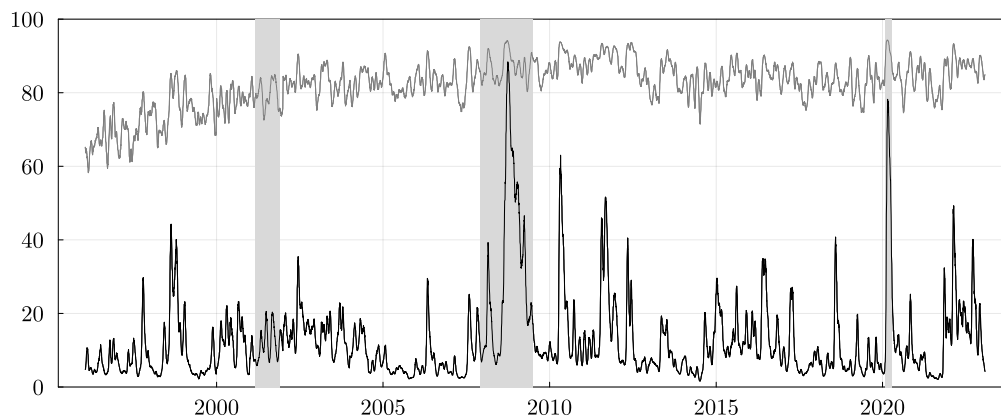


Figure 2. Network Connectedness Dynamics.

The figure depicts the time variation in the network connectedness $C(u, T)$ based on volatility linkages including a common correlation component (a grey line) and excluding a contemporaneous effect (a black line). The shaded areas denote the NBER recessions.

We apply the TVP-VAR model to daily risk-neutral volatilities on twenty exchange rates in our sample. In the empirical estimation, we define the short, medium, and long horizons as a 1-day to 1-week period, a 1-week to 1-month interval, and longer than 1 month, respectively. Furthermore, we consider two types of the time-varying covariance matrix $\hat{\Sigma}(u)$ used to compute the connectedness measures. First, we allow for the possibility of contemporaneous effects in volatility shocks. Second, we diagonalize the covariance matrix to remove the contemporaneous correlations. By diagonalizing the covariance matrix, we focus on network connections controlled for contemporaneous effects.

Figure 2 illustrates the network connectedness measure $C(u, T)$ for the two cases. We observe substantial differences in conditional dynamics depending on whether contemporaneous effects are present or removed. In particular, high unconditional correlations between risk-neutral currency volatilities induce a stable transmission of volatility shocks among individual currencies. As shown in the figure, this effect is strong and highly persistent over time, accounting for 80% of all connections in the adjacency matrix. However, it does not necessarily reflect a strong impact of option-based volatilities of individual currencies on each other, instead, it may be an artifact of a significant exposure of exchange rates to a global risk factor. In the context of the foreign exchange market, the natural candidates for this role could be the carry trade or the global volatility factors. Having removed contemporaneous effects, network connectedness becomes lower and exhibits countercyclical dynamics with prominent spikes during periods of tranquillity. For instance, we can clearly see surges in network connectedness during the Asian financial

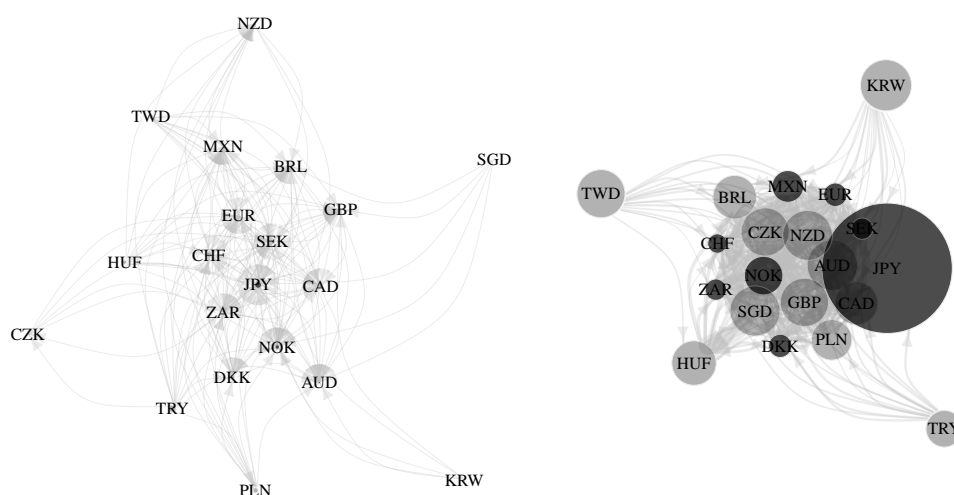


Figure 3. Transitory (left) and persistent (right) volatility networks: February 28, 2020

The left (right) figure depicts a transitory (persistent) network among option-implied currency volatilities based on connections of the transitory (permanent) nature of shocks. We remove the contemporaneous effects in volatility linkages by diagonalizing the covariance matrix. Arrows denote the direction of connections and the strength of lines denotes the strength of linkages. Grey (black) vertices denote currencies receiving (transmitting) more shocks than transmitting (receiving). The size of vertices indicates the net amount of shocks. To enhance the readability, links are drawn if intensities are above a predetermined threshold.

crisis in October 1997, the Russian financial crisis in 1998, the Global Financial Crisis in 2008-2009, the European sovereign debt crisis between 2010 and 2012, and the onset of the COVID outbreak in February 2020.

Although we provide evidence of substantial commonalities in network linkages, our free-from-correlation connectedness lends strong support for the presence of rich information in directional connections even after controlling for common variation. The novel contribution of this paper is to explore the information content of time-varying linkages in option-based currency volatilities beyond contemporaneous correlations through the lens of an asset pricing framework. The rest of the empirical analysis in Section 4 focuses on net-, to-, and from-directional connectedness measures (as described in Section 2.3) for the volatility network controlling for correlation effects.¹⁶

We now turn to present network structures at a granular level. Figure 3 demonstrates the network connections at the onset of the COVID outbreak on February 28, 2020. Com-

¹⁶Appendix provides the empirical results for network connectedness measures, which encompass contemporaneous correlations. Consistent with our intuition, the investment strategies formed on these volatility linkages are more correlated with the carry trade strategy. However, the excess returns of network portfolios remain economically and statistically significant after controlling for common currency factors, including the carry trade.

pared to the network structures at the beginning of the Global Financial Crisis illustrated in Figure 1, the transitory connections were weaker than the persistent ones during the COVID outbreak. Intuitively, this crisis was driven by a strong short-term shock in the global economy and hence almost no information is identified in transitory shocks beyond contemporaneous correlations. The most important lesson from Figures 1 and 3 is the stark differences in the status of individual currencies as being a net recipient or a net transmitter of shocks. Thus, these network structures emphasize how a currency's role may change not only over time but also in terms of persistence. We now move on to examining asset pricing implications of directional connections in a currency cross-section.

4.2 Net-directional Connectedness

Table 2 reports summary statistics of excess returns of five quintile portfolios ($\mathcal{P}_i : i = 1, \dots, 5$) and the long-short investment strategy buying \mathcal{P}_5 and selling \mathcal{P}_1 . It shows the results for horizon-specific net-directional portfolios. Several observations are noteworthy. First, the average return of a $\mathcal{N}(S)$ portfolio is 5.01% per annum, which is statistically different from zero at the 1% level. The “fx (%)” and “ir (%)” rows further indicate that this predictability stemming from network connections is primarily driven by predicting the spot exchange rates. For instance, the spread in the exchange rate component of excess returns of $\mathcal{N}(S)$ is 4.49% per annum, whereas the spread in the interest rate differentials is only 0.52% per annum. Also, there is no monotonicity in the forward premium as we move from \mathcal{P}_1 to \mathcal{P}_5 portfolios.

Second, the risk-adjusted performance of long-short portfolios deteriorates with the horizon of net-directional network risk. The annualized Sharpe ratio of network strategies gradually declines from 0.60 to 0.30 and 0.29 when using medium- and long- instead of short-term connections. These results indicate the downward-sloping term structure of net-directional network risk in the cross-section of currency returns. Our evidence complements the findings of Della Corte, Kozhan, and Neuberger (2021) demonstrating that the currency volatility risk premium decreases at longer horizons. Our paper also contributes to the literature on the price of variance risk in equity markets (Dew-Becker, Giglio, Le, and Rodriguez, 2017; Eraker and Wu, 2017; Johnson, 2017).

Third, the excess returns of the short-term network portfolio exhibit a large mean, a

Table 2. Net-directional Network Portfolios

This table presents descriptive statistics for quintile ($\mathcal{P}_i : i = 1, \dots, 5$) and long-short portfolios ($\mathcal{N}(\cdot)$) sorted by short- (S), medium- (M), and long-term (L) as well as total (T) net-directional connectedness. The portfolio \mathcal{P}_1 (\mathcal{P}_5) comprises currencies with the highest (lowest) network characteristic. The long-short portfolio buys \mathcal{P}_5 and sells \mathcal{P}_1 . Mean, standard deviation, and Sharpe ratio are annualized, but the t-statistic of mean, skewness, kurtosis, and the first-order autocorrelation are based on monthly returns. We also report the annualized mean of the exchange rate ($fx = -\Delta s^k$) and interest rate ($ir = i^k - i$) components of excess returns. The t-statistics are based on [Newey and West \(1987\)](#) standard errors. The sample is from January 1996 to January 2023.

	\mathcal{P}_1	\mathcal{P}_2	\mathcal{P}_3	\mathcal{P}_4	\mathcal{P}_5	$\mathcal{N}(S)$	\mathcal{P}_1	\mathcal{P}_2	\mathcal{P}_3	\mathcal{P}_4	\mathcal{P}_5	$\mathcal{N}(M)$
mean (%)	-1.27	-0.63	-0.74	-0.43	3.74	5.01	-1.46	0.35	0.47	0.35	0.92	2.38
t-stat	-0.65	-0.29	-0.40	-0.26	2.39	3.25	-0.75	0.19	0.28	0.19	0.54	1.72
fx (%)	-3.83	-1.62	-1.65	-1.90	0.66	4.49	-4.33	-1.04	-0.78	-0.83	-1.33	3.00
ir (%)	2.56	0.99	0.91	1.47	3.08	0.52	2.87	1.39	1.25	1.18	2.25	-0.62
net	0.04	0.00	-0.01	-0.02	-0.03	-0.07	0.05	-0.01	-0.02	-0.03	-0.04	-0.08
Sharpe	-0.12	-0.06	-0.08	-0.05	0.50	0.60	-0.15	0.04	0.06	0.04	0.11	0.30
std (%)	10.24	9.80	9.12	8.40	7.50	8.30	9.88	9.35	8.35	8.99	8.38	7.95
skew	-0.74	-0.54	-0.52	-0.37	0.01	0.74	-0.63	-0.37	-0.17	-0.56	-0.19	0.50
kurt	4.68	5.56	6.00	3.92	3.32	5.60	4.36	4.76	3.55	5.71	4.17	5.08
ac1	0.00	0.10	0.05	0.02	0.07	-0.05	0.04	0.01	-0.01	0.06	0.06	-0.10
	\mathcal{P}_1	\mathcal{P}_2	\mathcal{P}_3	\mathcal{P}_4	\mathcal{P}_5	$\mathcal{N}(L)$	\mathcal{P}_1	\mathcal{P}_2	\mathcal{P}_3	\mathcal{P}_4	\mathcal{P}_5	$\mathcal{N}(T)$
mean (%)	-1.57	1.01	0.09	0.31	0.72	2.29	-0.85	-0.30	-0.02	1.18	0.67	1.52
t-stat	-0.81	0.54	0.05	0.16	0.42	1.73	-0.45	-0.16	-0.01	0.66	0.41	1.11
fx (%)	-4.43	-0.63	-1.08	-0.88	-1.36	3.06	-3.63	-1.48	-1.23	-0.11	-1.83	1.79
ir (%)	2.86	1.64	1.17	1.19	2.08	-0.77	2.77	1.18	1.21	1.29	2.50	-0.27
net	0.05	-0.01	-0.02	-0.03	-0.04	-0.09	0.14	-0.03	-0.05	-0.08	-0.11	-0.25
Sharpe	-0.16	0.11	0.01	0.03	0.08	0.29	-0.09	-0.03	0.00	0.13	0.08	0.19
std (%)	9.91	8.84	8.21	9.29	8.77	7.94	9.99	8.97	8.63	8.97	8.35	8.00
skew	-0.69	-0.22	-0.24	-0.46	-0.37	0.50	-0.60	-0.29	-0.37	-0.34	-0.36	0.41
kurt	4.89	3.39	4.10	5.10	4.94	5.07	4.37	4.08	3.74	5.36	4.45	4.84
ac1	0.04	0.04	0.06	0.03	0.04	-0.07	0.01	0.05	0.10	0.04	0.03	-0.09

positive skew, and a sizeable kurtosis. The mean and volatility statistics imply that the improved Sharpe ratio originates mainly from higher returns and a moderate time variation. The positive skewness and excess kurtosis indicate that the distribution of portfolio returns formed on short-term net-directional connectedness has heavy tails with larger outliers in the right tail of the distribution. Indeed, analyzing the strategy's best and worst months, the portfolio experiences the three highest monthly returns of 9.00% in November 2021, 9.35% in September 2002, and 10.82% in October 2008, and the three lowest monthly returns of -5.66% in January 1998, -5.84% in August 2002, and -7.31% in October 2018.

4.3 To- and From-directional Connectedness

Table 3 presents descriptive statistics of the excess returns sorted on to-directional (Panel A) and from-directional (Panel B) connectedness. The table shows the results for

Table 3. To- and From-directional Network Portfolios

This table presents descriptive statistics for quintile ($\mathcal{P}_i : i = 1, \dots, 5$) and long-short portfolios ($\mathcal{T}(\cdot)$ and $\mathcal{F}(\cdot)$) sorted by short- (S), medium- (M), and long-term (L) as well as total (T) to-directional (Panel A) and from-directional (Panel B) connectedness. The portfolio $\mathcal{P}_1(\mathcal{P}_5)$ comprises currencies with the highest (lowest) network characteristic. The long-short portfolio buys \mathcal{P}_5 and sells \mathcal{P}_1 . Mean, standard deviation, and Sharpe ratio are annualized, but the t-statistic of mean, skewness, kurtosis, and the first-order autocorrelation are based on monthly returns. We also report the average network characteristic (net), the annualized mean of exchange rate ($fx = -\Delta s^k$) and interest rate ($ir = i^k - i$) components of excess returns. The t-statistics are based on Newey and West (1987) standard errors. The sample is from January 1996 to January 2023.

Panel A: To-directional network portfolios												
	\mathcal{P}_1	\mathcal{P}_2	\mathcal{P}_3	\mathcal{P}_4	\mathcal{P}_5	$\mathcal{T}(S)$	\mathcal{P}_1	\mathcal{P}_2	\mathcal{P}_3	\mathcal{P}_4	\mathcal{P}_5	$\mathcal{T}(M)$
mean (%)	-1.09	-0.99	-0.55	-0.21	3.74	4.84	-1.57	-0.34	-0.80	-0.61	4.14	5.70
t-stat	-0.54	-0.48	-0.30	-0.12	2.52	3.06	-0.75	-0.17	-0.43	-0.35	2.80	3.56
fx (%)	-3.67	-1.97	-1.55	-1.66	0.73	4.40	-4.03	-1.36	-1.86	-2.02	1.10	5.13
ir (%)	2.57	0.98	1.00	1.45	3.01	0.44	2.46	1.02	1.06	1.41	3.04	0.57
net	1.16	1.07	1.04	1.03	1.02	-0.14	1.49	1.22	1.15	1.11	1.06	-0.43
Sharpe	-0.10	-0.10	-0.06	-0.03	0.50	0.55	-0.15	-0.04	-0.09	-0.07	0.55	0.64
std (%)	10.50	9.64	9.34	8.31	7.47	8.72	10.71	9.47	9.18	8.33	7.55	8.86
skew	-0.79	-0.64	-0.33	-0.38	0.01	0.83	-0.85	-0.46	-0.48	-0.42	0.05	0.90
kurt	4.64	6.54	5.37	4.10	3.49	5.51	4.85	6.14	5.66	4.28	3.45	5.45
ac1	0.00	0.09	0.01	0.07	0.01	-0.09	0.00	0.08	0.01	0.05	0.01	-0.12
	\mathcal{P}_1	\mathcal{P}_2	\mathcal{P}_3	\mathcal{P}_4	\mathcal{P}_5	$\mathcal{T}(L)$	\mathcal{P}_1	\mathcal{P}_2	\mathcal{P}_3	\mathcal{P}_4	\mathcal{P}_5	$\mathcal{T}(T)$
mean (%)	-1.70	-0.74	0.13	-0.71	3.92	5.61	-1.11	-0.22	-1.35	-0.67	4.29	5.40
t-stat	-0.76	-0.37	0.07	-0.43	2.47	3.21	-0.53	-0.11	-0.72	-0.40	2.89	3.27
fx (%)	-4.17	-1.75	-0.92	-2.20	0.93	5.10	-3.72	-1.18	-2.35	-2.17	1.33	5.05
ir (%)	2.47	1.01	1.05	1.48	2.99	0.51	2.60	0.96	1.01	1.50	2.95	0.35
net	1.81	1.43	1.32	1.24	1.15	-0.67	1.37	1.15	1.10	1.07	1.04	-0.33
Sharpe	-0.16	-0.08	0.01	-0.08	0.51	0.64	-0.10	-0.02	-0.15	-0.08	0.57	0.61
std (%)	10.58	9.67	8.73	8.68	7.73	8.76	10.66	9.51	9.05	8.45	7.54	8.92
skew	-0.95	-0.49	-0.12	-0.44	-0.01	0.88	-0.92	-0.33	-0.40	-0.44	0.06	0.95
kurt	5.39	5.46	4.64	5.08	3.43	5.39	5.19	5.26	4.80	4.83	3.45	5.86
ac1	0.06	0.05	0.02	0.01	0.06	-0.05	0.02	0.07	0.01	0.07	0.01	-0.08
Panel B: From-directional network portfolios												
	\mathcal{P}_1	\mathcal{P}_2	\mathcal{P}_3	\mathcal{P}_4	\mathcal{P}_5	$\mathcal{F}(S)$	\mathcal{P}_1	\mathcal{P}_2	\mathcal{P}_3	\mathcal{P}_4	\mathcal{P}_5	$\mathcal{F}(M)$
mean (%)	-1.24	0.71	1.09	0.96	-0.78	0.47	-0.60	-0.40	0.96	0.99	0.04	0.64
t-stat	-0.67	0.37	0.61	0.55	-0.44	0.37	-0.29	-0.20	0.56	0.58	0.02	0.45
fx (%)	-3.46	-0.73	-0.37	-0.51	-3.10	0.36	-2.13	-1.36	-0.57	-0.76	-3.13	-1.00
ir (%)	2.22	1.44	1.46	1.47	2.32	0.11	1.53	0.97	1.53	1.75	3.17	1.64
net	1.08	1.07	1.07	1.06	1.06	-0.02	1.50	1.39	1.31	1.25	1.17	-0.33
Sharpe	-0.13	0.08	0.12	0.11	-0.09	0.07	-0.06	-0.04	0.12	0.11	0.00	0.08
std (%)	9.36	9.15	8.95	8.40	8.74	7.17	9.90	9.54	8.23	8.94	8.73	8.11
skew	-0.45	-0.34	-0.51	-0.27	-0.34	0.06	-0.51	-0.55	-0.43	0.08	-0.27	-0.08
kurt	3.97	4.61	5.68	4.63	3.48	3.76	4.46	5.80	4.66	4.22	3.43	3.65
ac1	0.04	0.09	0.01	0.05	0.05	0.00	0.07	0.11	0.04	-0.01	0.09	0.00
	\mathcal{P}_1	\mathcal{P}_2	\mathcal{P}_3	\mathcal{P}_4	\mathcal{P}_5	$\mathcal{F}(L)$	\mathcal{P}_1	\mathcal{P}_2	\mathcal{P}_3	\mathcal{P}_4	\mathcal{P}_5	$\mathcal{F}(T)$
mean (%)	-0.56	-0.45	1.58	0.56	-0.08	0.48	-0.78	-0.97	2.01	0.72	-0.12	0.66
t-stat	-0.28	-0.23	0.94	0.31	-0.04	0.32	-0.38	-0.49	1.19	0.47	-0.06	0.46
fx (%)	-2.07	-1.44	0.04	-1.16	-3.25	-1.18	-2.38	-2.17	0.49	-1.12	-2.88	-0.50
ir (%)	1.51	0.99	1.54	1.71	3.17	1.66	1.60	1.20	1.52	1.84	2.76	1.16
net	2.48	2.08	1.80	1.59	1.32	-1.16	1.32	1.25	1.20	1.16	1.12	-0.20
Sharpe	-0.06	-0.05	0.19	0.06	-0.01	0.06	-0.08	-0.10	0.24	0.09	-0.01	0.08
std (%)	9.51	9.33	8.19	9.07	9.09	7.94	9.88	9.72	8.42	8.32	8.76	8.03
skew	-0.44	-0.16	-0.41	-0.12	-0.29	-0.02	-0.62	-0.60	-0.35	-0.08	-0.14	0.16
kurt	4.46	4.50	4.37	4.87	3.89	3.62	5.46	4.81	5.09	3.71	3.32	4.18
ac1	0.07	0.05	0.06	-0.02	0.09	0.03	0.07	0.08	0.04	-0.06	0.11	0.02

horizon-specific network risk measures.

For the to-directional case, the spread between the excess returns of \mathcal{P}_5 and \mathcal{P}_1 portfo-

lios is increasing in the horizon and is statistically significant at the 1% level for all cases. Also, one can generally observe a monotonic pattern in the average excess returns of quintile portfolios, particularly for short-term to-directional connectedness. Consequently, currency portfolios based on the amount of transmitted shocks have annualized Sharpe ratios ranging from 0.55 to 0.64 for the short- and long-term horizon connectedness. All strategies display a positive skew of their excess returns. Interestingly, this performance primarily stems from the exchange rate predictability, while the interest rate differential contributes less. For the from-directional case, the results indicate no clear patterns in the descriptive statistics of currency network strategies. Although the average excess returns of quintile and long-short portfolios tend to be positive, they remain insignificant at all conventional confidence levels. This ultimately leads to much smaller Sharpe ratios compared to those from other strategies.

Overall, the results presented in Tables Table 2 and 3 suggest that the impact of a particular currency on the exchange rates of other countries is valuable for predicting future returns. Specifically, we document that the currencies transmitting more volatility shocks to others tend to earn smaller risk premiums. Unlike the carry trade strategy, we demonstrate that the stronger transmitters do not necessarily have the lowest interest rates. By connecting currency returns to network risk extracted from option-based volatilities, we shed light on the novel risk that drives exchange rates above and beyond the existing risks, macroeconomic country-specific conditions, and trade connections.

4.4 Benchmark Strategies and Diversification Gains

We now study the relationship between network portfolios and existing benchmarks. We begin by reporting in Table 4 summary statistics of the standard dollar, carry trade, volatility, volatility risk premium, and momentum strategies, as well as an equally weighted average of all currency benchmarks. The carry trade and momentum strategies exhibit the highest Sharpe ratios of 0.48 and 0.31, with the former having a statistically significant mean excess return. Both have a negative skewness, indicating the possibility of large losses. The last column shows no diversification gains from equally combining all strategies as indicated by no improvement in the Sharpe ratio and negative skewness of the “1/N” portfolio compared to the carry trade strategy.

Table 4. Benchmark Strategies: Summary Statistics

This table presents descriptive statistics (Panel A) and correlations (Panel B) of dollar (dol), carry trade (car), volatility (vol), volatility risk premium (vrp), momentum (mom) strategies, and equally weighted average of all benchmarks (1/N). Mean, standard deviation, and Sharpe ratio are annualized, but the t-statistic of mean, skewness, kurtosis, and the first-order autocorrelation are based on monthly returns. The t-statistics are based on [Newey and West \(1987\)](#) standard errors. The sample is from January 1996 to January 2023.

Panel A: Benchmark strategies						
	dol	car	vol	vrp	mom	1/N
mean (%)	0.14	5.37	2.61	0.98	2.84	2.39
t-stat	0.09	2.30	1.46	0.53	1.68	2.31
Sharpe	0.02	0.48	0.27	0.11	0.31	0.48
std (%)	7.88	11.22	9.64	9.15	9.20	5.02
skew	-0.40	-0.71	-0.18	0.07	-0.06	-0.52
kurt	4.52	4.67	4.64	4.92	3.40	5.12
ac1	0.07	0.05	-0.03	0.07	-0.02	0.05
Panel B: Correlations						
	dol	car	vol	vrp	mom	1/N
dol	1.00	0.32	0.58	-0.14	-0.15	0.57
car	0.32	1.00	0.40	0.25	0.03	0.80
vol	0.58	0.40	1.00	-0.20	-0.28	0.57
vrp	-0.14	0.25	-0.20	1.00	0.10	0.39
mom	-0.15	0.03	-0.28	0.10	1.00	0.26
1/N	0.57	0.80	0.57	0.39	0.26	1.00

Next, we examine how well the benchmark strategies can explain the network portfolios. We perform a two-step analysis. First, we compute the sample correlations between the excess returns of network portfolios and benchmark strategies. Second, we run contemporaneous regressions using network strategies as dependent variables and benchmark strategies as independent variables. [Table 5](#) reports the results of the two-stage exercise.

Focusing on the most profitable investments — short-term net-directional and four to-directional connectedness measures — several observations are worth discussing. First, these network strategies appear to be only weakly correlated with benchmark strategies. Interestingly, the excess returns are negatively correlated with the carry trade strategy, indicating a potential scope for diversification benefits when using the network portfolios in portfolio selections. Second, the relatively stronger correlations with dol and car directly translate into the borderline significant coefficients of these factors, whereas the remaining factors appear to have insignificant slopes. We can conclude that only a small portion of the excess returns formed on network measures reflects changes in interest rate differentials and common fluctuations of all exchange rates. Furthermore, this weak association with benchmark factors results in weak predictive power as measured by the low adjusted

Table 5. Network Portfolios and Benchmark Strategies

This table presents correlations (Panel A) and a contemporaneous regression (Panel B) of monthly returns of net-directional network portfolios ($\mathcal{N}(d) : d \in \{S, M, L, T\}$) on benchmark strategies — dollar (dol), carry trade (car), volatility (vol), volatility risk premium (vrp), and momentum (mom). Constants reported in the “alpha” row are expressed in percentage per annum. The numbers in rows with a grey font are t-statistics of estimates. The t-statistics are based on [Newey and West \(1987\)](#) standard errors. The last two rows report adjusted R^2 values (in percentage) and the number of observations. The sample is from January 1996 to January 2023.

Panel A: Correlations with trading strategies												
	$\mathcal{N}(S)$	$\mathcal{N}(M)$	$\mathcal{N}(L)$	$\mathcal{N}(T)$	$\mathcal{T}(S)$	$\mathcal{T}(M)$	$\mathcal{T}(L)$	$\mathcal{T}(T)$	$\mathcal{F}(S)$	$\mathcal{F}(M)$	$\mathcal{F}(L)$	$\mathcal{F}(T)$
dol	-0.26	-0.09	-0.03	-0.12	-0.28	-0.30	-0.25	-0.29	-0.13	-0.24	-0.14	-0.21
car	-0.26	-0.31	-0.31	-0.25	-0.27	-0.27	-0.25	-0.29	-0.07	0.12	0.15	0.06
vol	-0.23	-0.20	-0.18	-0.23	-0.25	-0.25	-0.22	-0.25	0.02	0.02	0.05	0.03
vrp	0.06	-0.07	-0.13	-0.08	0.08	0.07	0.05	0.07	-0.02	0.17	0.16	0.17
mom	0.14	0.15	0.14	0.18	0.15	0.15	0.15	0.16	-0.16	-0.06	-0.08	-0.13
Panel B: Returns of network portfolios on benchmark strategies												
	$\mathcal{N}(S)$	$\mathcal{N}(M)$	$\mathcal{N}(L)$	$\mathcal{N}(T)$	$\mathcal{T}(S)$	$\mathcal{T}(M)$	$\mathcal{T}(L)$	$\mathcal{T}(T)$	$\mathcal{F}(S)$	$\mathcal{F}(M)$	$\mathcal{F}(L)$	$\mathcal{F}(T)$
alpha	5.55	3.32	3.34	2.25	5.45	6.27	6.15	6.03	0.78	-0.19	-0.27	0.28
	3.43	2.40	2.56	1.56	3.39	3.92	3.45	3.71	0.61	-0.14	-0.19	0.21
dollar	-0.18	0.08	0.14	0.04	-0.19	-0.23	-0.17	-0.21	-0.19	-0.40	-0.28	-0.35
	-1.98	0.91	1.71	0.52	-2.00	-2.19	-1.96	-2.10	-2.65	-5.24	-3.58	-4.71
car	-0.17	-0.21	-0.21	-0.13	-0.19	-0.19	-0.18	-0.21	-0.03	0.10	0.11	0.03
	-2.20	-3.52	-3.78	-2.19	-2.16	-2.16	-2.07	-2.44	-0.59	1.75	2.08	0.49
vol	0.01	-0.07	-0.10	-0.13	0.00	0.01	0.01	0.02	0.09	0.17	0.12	0.18
	0.11	-0.84	-1.25	-1.45	-0.01	0.13	0.11	0.22	1.24	2.21	1.56	2.23
vrp	0.07	-0.02	-0.07	-0.07	0.09	0.08	0.07	0.10	0.00	0.12	0.10	0.14
	0.97	-0.28	-1.12	-1.06	1.12	1.00	0.86	1.07	0.04	2.00	1.90	1.91
mom	0.10	0.13	0.13	0.13	0.12	0.12	0.12	0.14	-0.12	-0.07	-0.08	-0.12
	1.51	2.20	2.21	2.19	1.59	1.67	1.68	1.82	-2.22	-1.20	-1.36	-2.03
$R^2(\%)$	12.35	12.78	14.06	11.16	14.16	14.92	11.61	15.79	5.93	14.50	9.92	12.74
Obs.	324	324	324	324	324	324	324	324	324	324	324	324

R^2 , which ranges from 11.16% to 15.79%. Third, the annualized alphas of the network strategies range from 5.45% to 6.27% and are larger than the average return of the corresponding portfolios due to a negative exposure to the dollar and carry trade factors. Overall, the results demonstrate that portfolios exploiting the information about the net amount of short-term volatility connections or the total amount of transmitted volatility shocks generate highly significant performance, both economically and statistically, which cannot be understood through the lens of the benchmarks.¹⁷

We further investigate the diversification benefits of network portfolios. For ease of presentation, we focus on the short-term net-directional case. We implement a naive strategy combining the network portfolio and one of the benchmarks at a time with 0.5-0.5 weights.

¹⁷We augment these results by replacing currency benchmarks with the five equity factors of [Fama and French \(1993\)](#) and momentum or the seven hedge fund factors of [Fung and Hsieh \(2004\)](#). As shown in Appendix, these alternative factors cannot explain the network portfolio alpha.

Table 6. Diversification Gains

This table presents the impact of adding a short-term net-directional strategy ($\mathcal{N}(S)$) to benchmark strategies — dollar (dol), carry trade (car), volatility (vol), volatility risk premium (vrp), and momentum (mom). We construct a naive 50%-50% portfolio of $\mathcal{N}(S)$ and one of benchmark strategies. The “1/N” column presents statistics of an equally weighted portfolio of all benchmarks and a network strategy. Mean, standard deviation, and Sharpe ratio are annualized, but the t-statistic of mean, skewness, kurtosis, and the first-order autocorrelation are based on monthly returns. The t-statistics are based on [Newey and West \(1987\)](#) standard errors. The last row shows the percentage increase in the Sharpe ratio of a diversified portfolio relative to the original benchmark strategy. The sample is from January 1996 to January 2023.

	dol	car	vol	vrp	mom	1/N
	+ $\mathcal{N}(S)$					
mean (% , annual)	2.57	5.19	3.81	2.99	3.93	3.70
t-stat	2.60	3.92	3.23	2.39	3.37	4.15
Sharpe	0.52	0.86	0.68	0.47	0.59	0.85
std (%)	4.91	6.07	5.60	6.34	6.61	4.37
skew	0.05	-0.05	0.58	1.02	0.24	0.15
kurt	3.44	4.19	4.84	8.74	5.13	3.93
ac1	0.02	0.11	0.02	0.04	-0.06	0.03
% Δ Sharpe	2850.98	78.76	151.29	340.69	92.36	78.12

Table 6 shows that the network portfolio generates significant diversification benefits. For instance, the allocation in $\mathcal{N}(S)$ and car generates a ratio of 0.86, which is 78.76% higher than the original carry trade. The resulting Sharpe ratios for other investments become even higher relative to the individual benchmarks, with the increase ranging from 92.36% for mom and to well above 340.69% for vrp.

Finally, we now perform the allocation analysis of selected portfolios: $\mathcal{N}(S)$, car, vol, vrp, and mom. Table 7 reports the fraction of months each investment strategy goes long (the “Buy” columns) or short (the “Sell” columns) in each currency. We also compute the fraction of months when the currency position in $\mathcal{N}(S)$ is different from the currency allocation in the benchmarks (the “Diff” columns). The bottom row shows the average fraction of “Diff” statistics across the currencies.

Table 7 demonstrates significant differences across strategies and countries. For instance, the network strategy on average buys or sells alternative currencies in 37%, 41%, 39%, and 41% of the time relative to the carry trade, volatility, volatility risk premium, and momentum. The countries whose allocations differ most in their distributions relative to $\mathcal{N}(S)$ are Japan and Switzerland for the carry trade, South Africa and Mexico for volatility, Mexico and South Africa for the volatility risk premium, and Japan and South Africa for momentum. Most notably, if we sort the currencies according to interest rate differentials,

Table 7. Allocation Analysis for the Network Portfolio and Benchmark Strategies

This table presents an allocation analysis of a short-term net-directional network portfolio ($\mathcal{N}(S)$) and carry trade (car), volatility (vol), volatility risk premium (vrp), and momentum (mom) strategies. The “Buy” and “Sell” columns report the fraction of months each currency belongs to the long and short positions of portfolios considered. The “Diff” column for each benchmark strategy reports the fraction of months the position for a particular currency is different from the one in $\mathcal{N}(S)$. The bottom row reports the average fraction across the currencies. The sample is from January 1996 to January 2023.

	$\mathcal{N}(S)$		car			vol			vrp			mom		
	Buy	Sell	Buy	Sell	Diff	Buy	Sell	Diff	Buy	Sell	Diff	Buy	Sell	Diff
Australia	0.17	0.14	0.00	0.00	0.31	0.17	0.02	0.43	0.09	0.25	0.50	0.18	0.14	0.49
Brazil	0.33	0.24	1.00	0.00	0.39	0.56	0.05	0.41	0.48	0.20	0.30	0.51	0.24	0.43
Canada	0.07	0.21	0.00	0.03	0.28	0.01	0.44	0.50	0.08	0.16	0.39	0.12	0.09	0.38
Czech Republic	0.10	0.18	0.00	0.10	0.05	0.14	0.05	0.10	0.09	0.33	0.19	0.18	0.12	0.12
Denmark	0.07	0.12	0.00	0.40	0.45	0.03	0.09	0.27	0.06	0.14	0.34	0.05	0.15	0.32
Euro Area	0.04	0.17	0.00	0.15	0.21	0.03	0.13	0.24	0.09	0.06	0.22	0.07	0.12	0.28
Hungary	0.20	0.21	0.46	0.00	0.34	0.40	0.00	0.36	0.13	0.32	0.34	0.22	0.19	0.32
Japan	0.25	0.22	0.00	0.91	0.77	0.18	0.19	0.59	0.22	0.21	0.58	0.22	0.42	0.68
Mexico	0.64	0.11	0.58	0.00	0.51	0.19	0.26	0.68	0.44	0.09	0.51	0.36	0.22	0.67
New Zealand	0.11	0.13	0.17	0.00	0.29	0.29	0.02	0.44	0.15	0.26	0.48	0.21	0.16	0.47
Norway	0.06	0.13	0.00	0.00	0.19	0.23	0.02	0.33	0.13	0.30	0.44	0.08	0.13	0.31
Poland	0.31	0.17	0.11	0.01	0.28	0.34	0.02	0.44	0.21	0.22	0.43	0.28	0.12	0.42
Singapore	0.10	0.31	0.00	0.41	0.15	0.00	0.98	0.41	0.09	0.06	0.20	0.14	0.14	0.27
South Africa	0.23	0.29	0.90	0.00	0.75	0.66	0.08	0.81	0.38	0.20	0.59	0.32	0.29	0.72
South Korea	0.68	0.08	0.00	0.00	0.29	0.04	0.39	0.36	0.36	0.11	0.24	0.24	0.13	0.18
Sweden	0.03	0.16	0.00	0.35	0.40	0.16	0.02	0.32	0.12	0.26	0.46	0.08	0.30	0.45
Switzerland	0.08	0.13	0.00	0.99	0.86	0.11	0.11	0.35	0.08	0.27	0.42	0.14	0.22	0.44
Taiwan	0.14	0.46	0.00	0.28	0.27	0.00	0.97	0.31	0.30	0.08	0.46	0.14	0.22	0.39
Turkey	0.37	0.31	1.00	0.00	0.21	0.39	0.14	0.36	0.53	0.15	0.22	0.28	0.37	0.36
United Kingdom	0.19	0.22	0.00	0.04	0.44	0.04	0.20	0.50	0.09	0.22	0.50	0.16	0.16	0.55
Average					0.37			0.41			0.39			0.41

we would have bought the South African rand (ZAR) in 90% of months and would have kept the Japanese yen (JPY) in the short position in 91% of months. Also, these currencies would have never entered an opposite lag. In contrast, our net-directional strategy buys and sells JPY in 25% and 22% of the time and ZAR in 23% and 29%.

4.5 Relating Network Portfolios to Liquidity and Volatility Risk

We now explore the contribution of two additional drivers of currency risk premia — global foreign exchange liquidity and volatility — in explaining the returns of network portfolios. We follow [Menkhoff et al. \(2012a\)](#) and consider several liquidity measures. First, we construct a global proxy for FX market illiquidity using the bid-ask spread (BAS) data of individual currencies.¹⁸ Second, we use the TED spread defined as the difference between three-month euro interbank deposits (LIBOR) and three-month Treasury bills as

¹⁸A global BAS measure in a month t is formally defined as:

$$BAS_t = \frac{1}{T_t} \sum_{\tau \in T_t} \left[\sum_{k \in K_\tau} \left(\frac{BAS_\tau^k}{K_\tau} \right) \right],$$

an illiquidity proxy in the funding market for carry trades. Third, we employ a liquidity measure of [Pástor and Stambaugh \(2003\)](#) (PS) for the U.S. stock market. Since we consider the U.S. investor, it is reasonable to account for liquidity risk in the home equity market. In relation to volatility risk, we first compute the proxy for global FX volatility (VOL) following the definition of [Menkhoff et al. \(2012a\)](#).¹⁹ Next, we use the VIX index, a risk-neutral expectation of stock market volatility, as a proxy for the risk aversion of U.S. investors to volatility risk. Finally, we consider the St. Louis Federal Reserve Bank Financial Stress Index (FSI) to capture the degree of financial stress in the U.S. economy. The FSI is constructed based on various interest rates, yield spreads, and other indicators.

Table 8 reports summary statistics of contemporaneous regressions of network portfolio returns on changes in measures of liquidity and volatility risk, one at a time. The estimated alphas remain economically and statistically significant in all cases, ranging from around 4.5% to 5% per annum. The slope coefficients for liquidity measures are not statistically different from zero at all conventional levels. It is worth emphasizing that the slope in the BAS regression flips the sign and has a larger (in absolute terms) t-statistic compared to the other two coefficients. Thus, volatility network risk is unrelated to illiquidity measures in the funding and equity markets and is positively associated with liquidity in FX, though the latter relationship is statistically weak. In contrast, the changes in volatility proxies positively predict the network portfolio returns. The coefficients for global FX volatility and FSI (VIX) appear to be highly (borderline) significant. This suggests that the network strategy performs well in times of heightened volatility risk.²⁰

Note that volatility and liquidity proxies are not tradable strategies. We construct the global liquidity and volatility portfolios following the procedure in [Della Corte et al. \(2016\)](#)

in which BAS_{τ}^k is the daily percentage BAS of a currency k on a day τ , K_{τ} is the number of available currencies on a day τ , and T_t is the number of days in a month t .

¹⁹The global VOL measure in a month t is formally defined as:

$$VOL_t = \frac{1}{T_t} \sum_{\tau \in T_t} \left[\sum_{k \in K_{\tau}} \left(\frac{|r_{\tau}^k|}{K_{\tau}} \right) \right],$$

in which $|r_{\tau}^k| = |\Delta s_{\tau}|$ is the absolute daily log return for a currency k on a day τ , K_{τ} is the number of available currencies on a day τ , and T_t is the number of days in a month t .

²⁰Relatedly, [Menkhoff et al. \(2012a\)](#) and [Bakshi and Panayotov \(2013\)](#) document a significant negative effect of volatility fluctuations on carry trade returns. Similarly, [Dahlquist and Hasseltoft \(2020\)](#) demonstrate a negative impact on the economic momentum strategy. In contrast, [Della Corte et al. \(2016\)](#) document a positive relationship between currency volatility risk premium and volatility risk, similar to our findings.

Table 8. Global FX Liquidity and Volatility Risk

This table presents a contemporaneous univariate regression of monthly returns of a short-term net-directional strategy ($\mathcal{N}(S)$) on the level of the PS liquidity measure and changes in the TED spread, the global foreign exchange liquidity and volatility measures, the St. Louis Federal Reserve Bank Financial Stress Index, and the VIX index. The last two columns use the tradable global liquidity and volatility factors, which are constructed based on the procedure in Della Corte et al. (2016), as predictors in the regression. Constants reported in the “alpha” row are expressed in percentage per annum. The numbers in rows with a grey font are t-statistics of estimates. The t-statistics are based on Newey and West (1987) standard errors. The last row reports adjusted R^2 values (in percentage). The sample is from January 1996 to January 2023.

	ΔTED	ΔBAS	PS	ΔVOL	ΔFSI	ΔVIX	BAS Factor	VOL Factor
alpha	4.47	4.88	4.87	4.90	4.92	4.92	4.97	5.31
	2.88	3.20	3.19	3.28	3.23	3.23	3.11	3.25
b_f	-0.00	8.32	-0.02	4.84	0.01	0.00	-0.11	-0.14
	-0.27	1.31	-0.83	4.15	2.75	1.85	-1.41	-1.84
$R^2(\%)$	0.02	0.88	0.16	6.48	3.37	2.42	1.69	2.94

and replicate the previous analysis with those factors.²¹ As the last two columns in Table 8 show, the network returns are only weakly negatively related to the tradable liquidity and volatility factors. The statistically significant alphas and low R^2 statistics further demonstrate that the volatility network premium cannot be explained by time-varying exposure of currency returns to global volatility and liquidity risk.

In sum, although it is difficult to disentangle volatility and liquidity effects, especially due to liquidity not being directly observable, the analysis provides insights into possible mechanisms driving our results. For instance, ambiguous results for liquidity proxies indicate that the network strategy is unlikely to be explained by variations in funding liquidity or limits to arbitrage. Further, the returns from the network portfolios are only weakly driven by the global risk aversion to liquidity and volatility risk as indicated by the weak significance of the BAS and VIX series. The regression using a global volatility (liquidity) factor as a predictor also shows little evidence of the possibility that network returns capture time-varying loadings on a global volatility (liquidity) shock, that is, fluctuations in risk aversion to volatility (liquidity) risk. Instead, our findings suggest risk aversion to financial stress as a possible explanation.

²¹For a global volatility (liquidity) factor, each month we estimate the regression of excess returns of individual currencies on constant and global volatility (liquidity) innovations using a 36-month rolling window. Having estimated the slope coefficients, we sort the currencies into quintile portfolios based on these betas. Then, we create a zero-cost strategy by buying (selling) the lowest (highest) beta quintile of currencies.

4.6 Weekly Frequency

Since the network estimates are available at a daily frequency, it is reasonable to test whether the key findings are sensitive to the frequency of rebalancing. We, therefore, construct network portfolios at a weekly frequency. Specifically, we use the daily network estimates from the core analysis and sample the end-of-week observations to construct long-short portfolios. Table 9 reports summary statistics of network portfolios (Panel A), correlations with different portfolios (Panel B), and regression outputs with network excess returns as a dependent variable and benchmarks as independent variables (Panel C).

Several observations are noteworthy. First, the Sharpe ratios of a short-term net-directional portfolio increase to 0.98. Note that the performance of the longer-term net-directional portfolios is significantly weaker, which suggests that volatility connections beyond one week possess weaker predictive power. Although this finding is not surprising given the non-overlapping periods of the one-week portfolio horizon and longer-term network connections. However, this evidence demonstrates the downward-sloping term structure of net-directional network risk, consistent with a monthly rebalancing. Second, the superior performance of the short-term net-directional strategy is driven by the to-directional component. Interestingly, the longer-term to-directional portfolios perform slightly weaker, indicating the weakly downward-sloping term structure of to-directional network risk. Third, the portfolio alphas strongly increase in magnitude and become highly significant, both economically and statistically: 9.29% per annum with a t-stat of 5.58 for $\mathcal{N}(S)$ and 9.58% per annum with a t-stat of 5.89 for $\mathcal{T}(S)$. In unreported results, we check that the remaining key conclusions of the main empirical analysis are robust to a weekly rebalancing procedure.

4.7 Transaction Costs

We perform two additional robustness checks. We begin by reporting the performance statistics for the network excess returns net of transaction costs. Since the bid-ask quotes for exchange rates are available from Barclays and Reuters, we incorporate those into the currency excess returns following [Menkhoff, Sarno, Schmeling, and Schrimpf \(2012b\)](#).²² It is worth noting that the bid-ask data are for quoted spreads and not effective spreads.

²²Please see Appendix C for more details on how we account for transaction costs.

Table 9. Weekly Frequency

This table presents a robustness analysis of currency strategies on a weekly frequency. The table reports descriptive statistics (Panel A), correlations (Panel B), and a contemporaneous regression (Panel C) of weekly returns of net-directional network portfolios on benchmark strategies — dollar (dol), carry trade (car), volatility (vol), volatility risk premium (vrp), and momentum (mom). In Panel A, mean, standard deviation, and Sharpe ratio are annualized, but the t-statistic of mean, skewness, kurtosis, and the first-order autocorrelation are based on weekly returns. In Panel C, constants reported in the “alpha” row are expressed in percentage per annum. The numbers in rows with a grey font are t-statistics of estimates. The t-statistics are based on [Newey and West \(1987\)](#) standard errors. The last two rows report adjusted R^2 values (in percentage) and the number of observations. The sample is from January 1996 to January 2023.

Panel A: Performance of network portfolios												
	$\mathcal{N}(S)$	$\mathcal{N}(M)$	$\mathcal{N}(L)$	$\mathcal{N}(T)$	$\mathcal{T}(S)$	$\mathcal{T}(M)$	$\mathcal{T}(L)$	$\mathcal{T}(T)$	$\mathcal{F}(S)$	$\mathcal{F}(M)$	$\mathcal{F}(L)$	$\mathcal{F}(T)$
mean (%)	8.64	4.89	4.50	4.78	9.04	8.57	8.10	8.77	0.30	0.16	1.02	0.98
t-stat	4.79	3.07	2.83	2.97	4.97	4.89	4.71	4.96	0.20	0.09	0.57	0.56
fx (%)	8.21	5.56	5.41	4.99	8.63	8.13	7.61	8.43	0.06	-1.47	2.69	-0.33
ir (%)	0.44	-0.67	-0.91	-0.20	0.41	0.44	0.49	0.34	0.24	1.63	-1.67	1.31
net	-0.07	-0.08	-0.09	-0.24	-0.14	-0.43	-0.66	-0.32	-0.02	-0.34	1.14	-0.19
Sharpe	0.98	0.59	0.54	0.57	1.02	0.95	0.93	1.00	0.04	0.02	0.12	0.11
std (%)	8.82	8.24	8.38	8.36	8.90	8.99	8.72	8.80	8.08	8.91	8.84	8.93
skew	0.17	-0.28	-0.27	-0.37	0.12	-0.08	-0.11	0.06	0.68	0.57	-0.29	0.61
kurt	11.69	11.22	10.54	10.77	11.30	11.40	10.17	10.82	9.65	8.72	8.45	8.60
ac1	0.03	0.00	0.01	0.00	0.00	-0.01	0.02	0.01	-0.04	-0.01	0.02	0.01
Panel B: Correlations with trading strategies												
	$\mathcal{N}(S)$	$\mathcal{N}(M)$	$\mathcal{N}(L)$	$\mathcal{N}(T)$	$\mathcal{T}(S)$	$\mathcal{T}(M)$	$\mathcal{T}(L)$	$\mathcal{T}(T)$	$\mathcal{F}(S)$	$\mathcal{F}(M)$	$\mathcal{F}(L)$	$\mathcal{F}(T)$
dol	-0.33	-0.19	-0.07	-0.19	-0.36	-0.35	-0.28	-0.34	0.00	-0.10	0.07	-0.13
car	-0.27	-0.30	-0.25	-0.25	-0.27	-0.26	-0.20	-0.27	0.09	0.24	-0.25	0.16
vol	-0.45	-0.37	-0.30	-0.37	-0.46	-0.46	-0.41	-0.46	0.12	0.09	-0.11	0.03
vrp	0.16	0.08	0.03	0.10	0.18	0.16	0.12	0.15	-0.09	0.08	-0.06	0.06
mom	0.30	0.24	0.18	0.24	0.33	0.36	0.30	0.34	-0.09	-0.09	0.10	-0.05
Panel C: Returns of network portfolios on benchmark strategies												
	$\mathcal{N}(S)$	$\mathcal{N}(M)$	$\mathcal{N}(L)$	$\mathcal{N}(T)$	$\mathcal{T}(S)$	$\mathcal{T}(M)$	$\mathcal{T}(L)$	$\mathcal{T}(T)$	$\mathcal{F}(S)$	$\mathcal{F}(M)$	$\mathcal{F}(L)$	$\mathcal{F}(T)$
alpha	9.29	5.92	5.65	5.62	9.58	9.09	8.61	9.40	0.08	-1.16	2.33	0.03
	5.58	3.93	3.69	3.64	5.89	5.84	5.43	5.88	0.05	-0.70	1.34	0.02
dollar	-0.08	0.09	0.25	0.10	-0.12	-0.11	-0.02	-0.08	-0.14	-0.32	0.29	-0.31
	-1.43	1.58	3.80	1.65	-1.85	-1.95	-0.37	-1.46	-2.48	-5.10	4.66	-4.60
car	-0.05	-0.09	-0.07	-0.05	-0.04	-0.02	0.02	-0.04	0.04	0.18	-0.18	0.13
	-0.97	-1.79	-1.37	-0.96	-0.83	-0.51	0.49	-0.86	0.73	3.17	-3.17	2.20
vol	-0.27	-0.27	-0.33	-0.30	-0.26	-0.28	-0.32	-0.27	0.11	0.14	-0.14	0.11
	-4.74	-4.54	-5.39	-5.02	-4.37	-5.30	-5.40	-5.10	1.99	2.25	-2.34	1.69
vrp	0.01	-0.03	-0.07	-0.03	0.02	-0.01	-0.05	-0.01	-0.06	0.07	-0.06	0.03
	0.20	-0.64	-1.18	-0.53	0.30	-0.20	-0.93	-0.15	-0.89	1.06	-0.86	0.48
mom	0.16	0.12	0.08	0.12	0.19	0.21	0.17	0.20	-0.04	-0.06	0.05	-0.03
	4.17	3.33	1.83	3.11	5.18	5.58	3.97	5.72	-0.92	-1.37	1.27	-0.64
R^2 (%)	23.51	18.24	14.80	16.93	26.52	27.45	20.90	26.23	3.27	11.09	10.78	7.29
Obs.	1365	1365	1365	1365	1365	1365	1365	1365	1365	1365	1365	1365

[Lyons et al. \(2001\)](#) suggest that the bid-ask spread data are based on the indicative spreads and, therefore, might be too high relative to actual effective ones. Following the existing literature (see, for example, [Goyal and Saretto \(2009\)](#), [Menkhoff, Sarno, Schmeling, and Schrimpf \(2012a, 2017\)](#), and [Colacito, Riddiough, and Sarno \(2020\)](#) among others), we

Table 10. Transaction Costs

This table presents descriptive statistics for long-short net-directional and to-directional network portfolios adjusted for transaction costs. Mean, standard deviation, and Sharpe ratio are annualized, but the t-statistic of mean, skewness, kurtosis, and the first-order autocorrelation are based on monthly returns. The t-statistics are based on [Newey and West \(1987\)](#) standard errors. The sample is from January 1996 to January 2023.

	$\mathcal{N}(S)$	$\mathcal{N}(M)$	$\mathcal{N}(L)$	$\mathcal{N}(T)$	$\mathcal{T}(S)$	$\mathcal{T}(M)$	$\mathcal{T}(L)$	$\mathcal{T}(T)$
mean (%)	4.07	1.55	1.68	0.52	3.58	4.26	4.14	4.09
t-stat	2.53	1.09	1.25	0.37	2.15	2.58	2.34	2.39
Sharpe	0.48	0.19	0.22	0.07	0.41	0.48	0.48	0.46
std (%)	8.40	7.96	7.82	8.00	8.75	8.82	8.65	8.90
skew	0.90	0.49	0.42	0.35	0.97	1.04	0.89	1.04
kurt	6.46	4.57	4.48	4.27	6.26	6.29	5.37	6.41
ac1	0.00	-0.06	-0.03	-0.06	-0.02	-0.06	0.00	-0.03

employ 50% of quoted bid-ask spreads in our calculations.²³

Table 10 reports summary statistics of the excess returns of currency network portfolios adjusted for transaction costs. In comparison with the results shown in Tables 2 and 3, the Sharpe ratio of the $\mathcal{N}(S)$ portfolio declines from 0.60 to 0.48. The to-directional network portfolios experience a comparable drop in their performances, with the Sharpe ratios ranging from 0.41 to 0.48. Hence, although the returns are somewhat lower after accounting for transaction costs, the network portfolios still exhibit both economically and statistically significant performance.

4.8 Subsamples

As an additional robustness check, we refute the concern that our results may be driven by a particular period of time by looking at network portfolios across subsamples. The availability and the amount of currency options vary over time and countries, with sparser data during the first decade of our sample. It has been also known that the common currency strategies have experienced a significant decline in their performance after the 2007-2008 financial crisis. Motivated by these observations, we report results for the subsample just before the first episode of the financial crisis (January 1996 to June 2007) and the subsequent period (July 2007 to January 2023).

Table 11 reports the results. The benchmark strategies exhibit considerable differences in their performance across subsamples. In particular, the carry trade and momentum

²³[Gilmore and Hayashi \(2011\)](#) suggest that the effective bid-ask spreads could be even lower than 50%, while [Cespa, Gargano, Riddiough, and Sarno \(2021\)](#) suggest a 25% rule for the data from 2011.

Table 11. Subsamples

This table presents descriptive statistics of net-directional and to-directional network portfolios (Panel A) and benchmark strategies (Panel B) for subsamples from January 1996 to June 2007 and from July 2007 to January 2023. Mean, standard deviation, and Sharpe ratio are annualized, but the t-statistic of mean, skewness, kurtosis, and the first-order autocorrelation are based on monthly returns. The t-statistics are based on [Newey and West \(1987\)](#) standard errors.

Panel A: Network strategies								
	1996.1-2007.6				2007.7-2023.1			
	$\mathcal{N}(S)$	$\mathcal{N}(M)$	$\mathcal{N}(L)$	$\mathcal{N}(T)$	$\mathcal{N}(S)$	$\mathcal{N}(M)$	$\mathcal{N}(L)$	$\mathcal{N}(T)$
mean (%)	5.36	1.72	1.61	1.78	4.75	2.86	2.79	1.33
t-stat	2.21	0.80	0.73	0.81	2.41	1.60	1.63	0.76
Sharpe	0.59	0.18	0.17	0.19	0.61	0.42	0.41	0.20
std (%)	9.02	9.36	9.31	9.43	7.75	6.75	6.78	6.80
skew	0.57	0.65	0.71	0.41	0.91	0.23	0.11	0.34
kurt	4.54	4.52	4.57	4.03	6.73	4.90	4.87	5.28
ac1	-0.10	-0.21	-0.16	-0.18	0.00	0.05	0.06	0.02
	1996.1-2007.6				2007.7-2023.1			
	$\mathcal{T}(S)$	$\mathcal{T}(M)$	$\mathcal{T}(L)$	$\mathcal{T}(T)$	$\mathcal{T}(S)$	$\mathcal{T}(M)$	$\mathcal{T}(L)$	$\mathcal{T}(T)$
mean (%)	5.66	5.63	5.91	5.74	4.93	5.76	5.39	5.82
t-stat	2.01	2.28	2.30	1.94	2.42	2.76	2.35	2.69
Sharpe	0.59	0.59	0.62	0.60	0.61	0.69	0.66	0.70
std (%)	9.60	9.60	9.54	9.56	8.04	8.30	8.17	8.36
skew	0.66	0.67	0.65	0.66	1.06	1.15	1.14	1.29
kurt	4.42	4.35	4.37	4.42	6.60	6.63	6.47	7.58
ac1	-0.12	-0.19	-0.14	-0.15	-0.03	-0.05	0.05	-0.03
Panel B: Benchmark strategies								
	1996.1-2007.6				2007.7-2023.1			
	car	vol	vrp	mom	car	vol	vrp	mom
mean (%)	11.96	3.64	2.84	8.02	0.54	1.85	-0.39	-0.95
t-stat	3.46	1.16	0.93	2.86	0.18	0.87	-0.17	-0.49
Sharpe	1.07	0.35	0.27	0.82	0.05	0.21	-0.05	-0.11
std (%)	11.19	10.53	10.47	9.81	11.07	8.97	8.04	8.59
skew	-0.62	0.39	-0.42	-0.11	-0.84	-0.88	0.77	-0.11
kurt	3.98	3.52	3.51	3.05	5.22	5.77	7.26	3.75
ac1	-0.03	0.01	0.04	0.02	0.08	-0.07	0.11	-0.10

portfolios produce annualized Sharpe ratios of 1.07 and 0.82 in the first period and only 0.05 and -0.11 in the second period. This deterioration in performance is also visible in the case of volatility-related strategies, though their average returns are statistically insignificant at conventional confidence levels in both samples.²⁴ In contrast, the performance of network portfolios remains strong before and after the financial crisis. Specifically, they

²⁴Our results are not inconsistent with the vrp profitability documented by [Della Corte et al. \(2016\)](#). The difference between our and their performance statistics originates from the definition of the volatility risk premium. In their paper, the authors work with the one-year volatility swaps, whereas we choose to work with a more common monthly horizon to be consistent with network risk measures estimated from one-month risk-neutral volatilities.

produce Sharpe ratios of around 0.60 before mid-2007, whereas their risk-adjusted returns even slightly increase and range from 0.61 to 0.70 on the annual basis after mid-2007.

4.9 Additional Exercises

We experiment with alternative methods to estimate network connectedness. First, we apply the TVP-VAR model to option-implied variances of individual currencies and construct the network portfolios for variance linkages. As shown in Table 12, the results remain substantially unchanged. The transitory net-directional network portfolio earns large raw and risk-adjusted excess returns, both in economic and statistical terms, and provides excellent diversification benefits as indicated by weak (and negative) correlations with benchmark strategies. Also, the to-directional connectedness component of asymmetric linkages contains strong predictive power.

Second, we replicate our analysis on realized volatilities estimated on the one-month rolling window basis. This exercise evaluates the incremental contribution of using the ex-ante expectation of currency volatilities synthesized from currency options. Table 13 shows that the forward-looking information of options data becomes instrumental for our results. Indeed, the network connectedness measures estimated from the realized volatilities contain almost no predictive power. This is also where our study goes beyond [Menkhoff, Sarno, Schmeling, and Schrimpf \(2012a\)](#). Although global foreign exchange volatility risk is useful for predicting currency returns and is associated with the carry trade strategy, we do not find useful predictive information in how realized volatilities of individual currencies relate to each other. In contrast, making effective use of information from currency options markets helps us discover novel predictive information in investor expectations about future currency fluctuations. We hope that the findings of this paper will advance the usage of options data in the foreign exchange market.

5 Asset Pricing

This section presents the cross-sectional asset-pricing tests performed on the excess returns of network portfolios. Motivated by the previous results, we begin our investigation by focusing on the cross-section of currency returns sorted by the short-term net-directional connectedness measures that control for contemporaneous correlations. To better under-

Table 12. Network Portfolios: Option-Implied Variances

This table presents a robustness analysis of currency strategies formed on network connectedness measures, which are estimated from option-implied variances. The table reports descriptive statistics of net-directional and to-directional network portfolios (Panel A), correlations (Panel B), and a contemporaneous regression (Panel C) of monthly returns of network portfolios on benchmark strategies - dollar (dol), carry trade (car), volatility (vol), volatility risk premium (vrp), and momentum (mom). In Panel A, mean, standard deviation, and Sharpe ratio are annualized, but the t-statistic of mean, skewness, kurtosis, and the first-order autocorrelation are based on monthly returns. We also report the annualized mean of the exchange rate ($fx = -\Delta s^k$) and interest rate ($ir = i^k - i$) components of excess returns. In Panel C, constants reported in the “alpha” row are expressed in percentage per annum. The numbers in rows with a grey font are t-statistics of estimates. The t-statistics are based on [Newey and West \(1987\)](#) standard errors. The last two rows report adjusted R^2 values (in percentage) and the number of observations. The sample is from January 1996 to January 2023.

Panel A: Performance of network portfolios												
	$\mathcal{N}(S)$	$\mathcal{N}(M)$	$\mathcal{N}(L)$	$\mathcal{N}(T)$	$\mathcal{T}(S)$	$\mathcal{T}(M)$	$\mathcal{T}(L)$	$\mathcal{T}(T)$	$\mathcal{F}(S)$	$\mathcal{F}(M)$	$\mathcal{F}(L)$	$\mathcal{F}(T)$
mean (%)	5.32	1.86	1.12	2.68	5.20	5.12	5.02	4.93	1.06	0.99	0.35	0.29
t-stat	3.44	1.43	0.90	1.99	3.65	3.58	3.56	3.39	0.77	0.70	0.25	0.21
fx (%)	3.38	1.12	0.46	1.52	3.15	3.01	2.84	2.91	0.65	-0.56	-1.09	-0.86
ir (%)	1.94	0.74	0.66	1.16	2.05	2.12	2.18	2.02	0.40	1.55	1.45	1.15
net	-0.06	-0.07	-0.07	-0.21	-0.14	-0.36	-0.56	-0.28	-0.02	-0.31	-1.03	-0.18
Sharpe	0.67	0.25	0.16	0.36	0.63	0.61	0.60	0.59	0.14	0.13	0.05	0.04
std (%)	7.98	7.42	7.15	7.44	8.27	8.34	8.31	8.39	7.28	7.88	7.62	7.77
skew	0.77	0.16	0.07	0.06	0.37	0.26	0.42	0.49	0.38	0.37	0.28	0.36
kurt	6.70	5.19	5.13	5.45	5.22	5.27	5.35	5.46	4.13	4.36	3.91	4.58
ac1	-0.05	-0.03	-0.03	-0.03	-0.10	-0.11	-0.09	-0.09	0.02	0.02	-0.01	0.02
Panel B: Correlations with trading strategies												
	$\mathcal{N}(S)$	$\mathcal{N}(M)$	$\mathcal{N}(L)$	$\mathcal{N}(T)$	$\mathcal{T}(S)$	$\mathcal{T}(M)$	$\mathcal{T}(L)$	$\mathcal{T}(T)$	$\mathcal{F}(S)$	$\mathcal{F}(M)$	$\mathcal{F}(L)$	$\mathcal{F}(T)$
dol	-0.18	0.01	0.07	-0.04	-0.21	-0.23	-0.16	-0.21	-0.25	-0.27	-0.21	-0.24
car	-0.01	-0.02	-0.04	-0.04	-0.06	-0.05	-0.02	-0.08	-0.09	0.08	0.13	0.04
vol	-0.17	-0.19	-0.20	-0.22	-0.24	-0.28	-0.25	-0.25	0.01	0.02	0.05	0.03
vrp	0.20	0.05	0.05	0.07	0.17	0.20	0.10	0.16	-0.01	0.17	0.08	0.12
mom	0.16	0.19	0.18	0.21	0.18	0.23	0.25	0.21	-0.05	-0.02	-0.03	-0.07
Panel C: Returns of network portfolios on benchmark strategies												
	$\mathcal{N}(S)$	$\mathcal{N}(M)$	$\mathcal{N}(L)$	$\mathcal{N}(T)$	$\mathcal{T}(S)$	$\mathcal{T}(M)$	$\mathcal{T}(L)$	$\mathcal{T}(T)$	$\mathcal{F}(S)$	$\mathcal{F}(M)$	$\mathcal{F}(L)$	$\mathcal{F}(T)$
alpha	4.99	1.96	1.42	2.75	5.13	4.96	4.74	4.88	0.96	0.17	-0.50	-0.22
dollar	3.20	1.40	1.07	1.89	3.34	3.30	3.13	3.11	0.73	0.13	-0.39	-0.17
car	-0.12	0.16	0.25	0.12	-0.10	-0.11	-0.03	-0.09	-0.34	-0.43	-0.36	-0.38
vol	-1.37	2.37	3.96	1.68	-1.27	-1.30	-0.32	-1.22	-4.33	-5.84	-4.51	-5.16
vrp	-0.01	0.02	0.00	0.01	-0.01	0.00	0.05	-0.03	-0.04	0.06	0.11	0.03
mom	-0.07	0.35	-0.06	0.10	-0.19	0.01	0.58	-0.34	-0.67	0.94	1.79	0.41
alpha	-0.02	-0.21	-0.23	-0.19	-0.11	-0.13	-0.18	-0.11	0.18	0.20	0.15	0.20
alpha	-0.26	-3.33	-3.85	-2.96	-1.29	-1.63	-2.15	-1.28	2.26	2.32	1.63	2.64
alpha	0.15	0.00	0.01	0.01	0.12	0.13	0.02	0.11	0.00	0.12	0.02	0.10
alpha	1.59	0.00	0.20	0.20	1.38	1.46	0.19	1.28	0.02	1.91	0.41	1.42
alpha	0.10	0.11	0.10	0.13	0.11	0.14	0.17	0.14	-0.03	-0.03	-0.04	-0.06
alpha	1.66	1.93	1.97	2.13	1.55	2.00	2.42	1.86	-0.57	-0.48	-0.60	-1.07
$R^2(\%)$	8.18	7.94	10.64	8.51	9.69	13.12	10.79	10.41	10.13	15.12	11.26	12.29
Obs.	324	324	324	324	324	324	324	324	324	324	324	324

stand the novel network risk beyond the common fluctuations, we also consider the corresponding cross-section of currency returns sorted by the short-term net-directional connectedness measures including contemporaneous correlations.

Table 13. Network Portfolios: Realized Volatilities

This table presents a robustness analysis of currency portfolios sorted on network risk measures, which are estimated from realized volatilities. The table reports descriptive statistics of the short-term net-, to-, and from-directional network portfolios. In Panel A, mean, standard deviation, and Sharpe ratio are annualized, but the t-statistic of mean, skewness, kurtosis and the first-order autocorrelation are based on monthly returns. We also report the annualized mean of the exchange rate ($fx = -\Delta s^k$) and interest rate ($ir = i^k - i$) components of excess returns. The t-statistics are based on [Newey and West \(1987\)](#) standard errors. The sample is from January 1996 to January 2023.

Panel A: Performance of network portfolios												
	$\mathcal{N}(S)$	$\mathcal{N}(M)$	$\mathcal{N}(L)$	$\mathcal{N}(T)$	$\mathcal{T}(S)$	$\mathcal{T}(M)$	$\mathcal{T}(L)$	$\mathcal{T}(T)$	$\mathcal{F}(S)$	$\mathcal{F}(M)$	$\mathcal{F}(L)$	$\mathcal{F}(T)$
mean (%)	0.55	0.51	1.17	0.24	1.41	1.05	0.76	1.57	1.41	1.83	0.29	1.98
t-stat	0.38	0.35	0.82	0.18	1.03	0.76	0.52	1.13	0.98	1.16	0.17	1.18
fx (%)	0.83	0.11	0.78	-0.02	1.82	1.47	1.01	2.00	1.18	1.46	0.77	1.98
ir (%)	-0.28	0.40	0.39	0.26	-0.41	-0.42	-0.25	-0.43	0.23	0.38	-0.48	0.00
net	-0.10	0.17	0.25	0.54	-0.28	-0.91	-1.49	-0.74	-3.74	-0.74	-0.04	-0.53
Sharpe	0.07	0.07	0.16	0.03	0.18	0.14	0.10	0.20	0.18	0.23	0.04	0.25
std (%)	8.22	7.45	7.37	7.58	7.73	7.75	7.77	7.80	7.86	8.07	7.85	7.79
skew	0.38	-0.50	-0.11	-0.30	0.60	0.66	0.52	0.61	-0.50	-0.49	-0.24	0.29
kurt	5.45	5.18	6.37	5.17	4.90	5.52	5.27	5.27	5.00	5.52	6.20	5.25
ac1	-0.03	0.02	-0.03	-0.05	-0.06	-0.05	-0.02	-0.05	-0.05	-0.03	0.03	0.06
Panel B: Correlations with trading strategies												
	$\mathcal{N}(S)$	$\mathcal{N}(M)$	$\mathcal{N}(L)$	$\mathcal{N}(T)$	$\mathcal{T}(S)$	$\mathcal{T}(M)$	$\mathcal{T}(L)$	$\mathcal{T}(T)$	$\mathcal{F}(S)$	$\mathcal{F}(M)$	$\mathcal{F}(L)$	$\mathcal{F}(T)$
dol	-0.39	0.28	0.16	0.18	-0.39	-0.37	-0.37	-0.37	0.13	0.09	0.10	-0.01
car	-0.33	0.29	0.18	0.18	-0.35	-0.36	-0.36	-0.35	-0.07	0.09	0.14	-0.09
vol	-0.55	0.49	0.46	0.47	-0.55	-0.52	-0.54	-0.53	0.26	0.26	0.32	0.12
vrp	0.11	0.00	0.04	0.02	0.10	0.11	0.10	0.10	-0.10	0.03	0.04	0.01
mom	0.17	-0.17	-0.17	-0.17	0.18	0.15	0.18	0.16	-0.24	-0.17	-0.15	-0.10

5.1 Methodology

Cross-sectional asset pricing tests are based on a stochastic discount factor (SDF) approach ([Cochrane, 2005](#)). In our application, we adopt the setting of [Lustig, Roussanov, and Verdelhan \(2011\)](#) for the network portfolios of our paper. In the absence of arbitrage opportunities, the excess returns rx_{t+1}^j of a portfolio j have a zero price and satisfy the following Euler equation:

$$\mathbb{E}_t \left(M_{t+1} rx_{t+1}^j \right) = 0, \tag{12}$$

in which M_{t+1} is the SDF. Following a common approach in the literature, we consider the linear specification of M_{t+1} :

$$M_{t+1} = 1 - b'(f_{t+1} - \mu_f), \tag{13}$$

in which f_{t+1} is the vector of pricing factors, b is the vector of SDF loadings, μ_f is the vector of factor means.²⁵ Combining Eq. (12)-(13), one can obtain a beta pricing model $\mathbb{E}_t \left(rx_{t+1}^j \right) = \lambda' \beta^j$, in which λ is the vector of the factor risk prices, and β^j is the vector of the risk quantities. The latter ones are also the regression coefficients of excess returns rx_{t+1}^j on the risk factors f_{t+1} . Further, the SDF loadings and factor risk prices are related to each other via the equation $\lambda = \Sigma_f b$, where $\Sigma_f = \mathbb{E}_t \left[(f_{t+1} - \mu_f)(f_{t+1} - \mu_f)'\right]$ is the variance-covariance matrix of risk factors.

We test a variety of linear factor models for the cross-section of network portfolios. For each model specification, we estimate the factor loadings via the one-step generalized method of moments (GMM) with the identity weighting matrix (Hansen, 1982). We simultaneously estimate the unknown factor means by adding the corresponding restrictions to a set of moments for the pricing errors. Since we are interested in testing whether a particular linear model explains the cross-section of expected currency excess returns, we implement a GMM estimation based on unconditional moments without instruments. Having estimated SDF loadings, we recover the risk prices from the identity $\lambda = \Sigma_f b$ and calculate their standard errors using the Delta method. The t-statistics of b 's and λ 's are based on Newey and West (1987) standard errors. We evaluate the fit of linear pricing models by using three statistics: the cross-sectional R^2 , root mean squared pricing error (RMSE), and the Hansen and Jagannathan (1997) distance (HJ_{dist}). We further calculate the simulated p-values for testing the null hypothesis that the pricing errors equal zero, i.e. HJ_{dist} equals zero. Following Jagannathan and Wang (1996) and Kan and Robotti (2008), we obtain the simulated p-values by using a weighted sum of independent random variables from $\chi^2(1)$ distribution.²⁶

5.2 Principal Component Analysis on Network Portfolios

Before performing formal cross-sectional asset pricing tests, we investigate whether average network excess returns stemming from short-term net-directional connectedness can be associated with a small group of risk factors. Following Lustig, Roussanov, and Verdelhan (2011), we conduct a principal component (PC) decomposition of currency net-

²⁵Other prominent examples considering a linear SDF specification include Menkhoff, Sarno, Schmeling, and Schrimpf (2012a), Della Corte, Ramadorai, and Sarno (2016), Colacito, Riddiough, and Sarno (2020) and Della Corte, Kozhan, and Neuberger (2021) among many others.

²⁶Appendix B provides a detailed description of the GMM estimation and test statistics.

Table 14. Principal Components: Short-term Net-directional Network Portfolios

This table presents the loadings of the principal components ($PC_i : i = 1, \dots, 5$) for quintile portfolios ($\mathcal{P}_i : i = 1, \dots, 5$) sorted by short-term net-directional connectedness extracted from volatility linkages including (Panel A) or excluding (Panel B) contemporaneous correlations. Each panel also reports correlations of principal components with a long-short network portfolio ($\mathcal{N}(S)$) and benchmark strategies — dollar (dol), carry trade (car), volatility (vol), volatility risk premium (vrp), and momentum (mom). The sample is from January 1996 to January 2023.

Panel A: Including contemporaneous correlations												
	PC loadings						Correlations					
	\mathcal{P}_1	\mathcal{P}_2	\mathcal{P}_3	\mathcal{P}_4	\mathcal{P}_5	CV	$\mathcal{N}(S)$	dol	car	vol	vrp	mom
PC1	0.53	0.52	0.44	0.38	0.34	76.50	-0.41	1.00	0.30	0.57	-0.15	-0.15
PC2	-0.53	-0.34	0.22	0.67	0.31	84.78	0.62	0.05	0.43	0.19	0.20	-0.03
PC3	0.05	-0.03	-0.51	-0.20	0.84	92.25	0.55	0.01	-0.08	-0.01	0.03	0.13
PC4	-0.24	-0.10	0.69	-0.61	0.29	97.42	0.30	0.01	0.14	0.05	0.20	-0.03
PC5	-0.62	0.77	-0.13	-0.04	-0.02	100.00	0.24	0.00	0.01	-0.05	-0.04	0.09
Panel B: Excluding contemporaneous correlations												
	PC loadings						Correlations					
	\mathcal{P}_1	\mathcal{P}_2	\mathcal{P}_3	\mathcal{P}_4	\mathcal{P}_5	CV	$\mathcal{N}(S)$	dol	car	vol	vrp	mom
PC1	0.48	0.51	0.47	0.41	0.34	76.99	-0.30	1.00	0.32	0.59	-0.15	-0.15
PC2	0.85	-0.13	-0.26	-0.38	-0.20	87.14	-0.82	-0.03	0.38	0.10	0.06	-0.09
PC3	0.14	-0.60	-0.28	0.36	0.64	92.94	0.40	0.02	0.12	0.09	0.15	0.09
PC4	0.13	-0.31	0.09	0.67	-0.65	97.07	-0.39	-0.01	-0.09	-0.01	-0.05	0.02
PC5	0.03	-0.52	0.79	-0.32	0.03	100.00	0.00	0.00	0.01	0.04	0.07	0.02

work portfolios formed on volatility linkages including and excluding contemporaneous effects. Further, we study the correlations of principal components with the network and benchmark strategies.

Table 14 presents the results. There are several common and distinctive features of the two cross-sections. First, the PC loadings indicate a strong factor structure in both groups of network cross-sections. The first principal component (PC1) accounts for most of the time-variation in quintile portfolios and has similar loadings across the five portfolios. The second principal component (PC2) in turn displays a pronounced monotonic pattern in loadings as we move from \mathcal{P}_1 to \mathcal{P}_5 : the increasing pattern for aggregate linkages and the decreasing tendency for causal connections. Second, the first two principal components explain around 84% (87%) of the common variation in network portfolios formed on connections with (without) a common correlation component. Further, they exhibit similar correlations with risk factors. PC1 is perfectly correlated with the dollar factor in both cases. PC2 exhibits the strongest correlation with the network portfolio, though the relationship is of the opposite sign in the two cases. In relative terms, when controlling for

contemporaneous effects, the correlation of PC2 with $\mathcal{N}(S)$ is strongly dominant, whereas PC2 from network portfolios formed on volatility linkages with common correlations more evenly correlates with $\mathcal{N}(S)$ and the carry trade factor. Finally, the starkest difference between the two portfolio groups is related to loadings of the third principal component (PC3) that show no visible pattern in Panel A but tend to display monotonicity in Panel B. In the latter case, PC3 has the strongest relationship with the network risk factor.

Overall, the results in Table 14 suggest that the network-sorted portfolios can indeed be summarized by a small number of risk factors. We can approximate the first using the average returns across spot currency portfolios and interpret it as a “level” factor. We can approximate the second using the spread between \mathcal{P}_5 and \mathcal{P}_1 portfolios and interpret it as a “slope” factor. For the cross-section sorted on network connectedness controlling for contemporaneous correlations, the results are suggestive of an additional “slope” factor, which is strongly correlated with the carry trade.

5.3 Cross-Sectional Regressions

We now turn to the formal investigation of network portfolios following the methodology outlined in Section 5.1. Motivated by the principal component analysis in Section 5.2, we consider (A1) a variety of two-factor linear models for the cross-section of excess returns sorted on net-directional connectedness including a common correlation component in volatility linkages and (A2) a variety of two- and three-factor linear models for the test excess returns sorted on net-directional connectedness excluding a contemporaneous effect. In particular, the two-factor SDFs has dol as the first factor plus a second factor, including car, vol, vrp, mom, or $\mathcal{N}(S)$ one at a time. For the three-factor SDFs, we start with the two factors, dol and $\mathcal{N}(S)$, and then consider various third factors, including car, vol, vrp, or mom.

Table 15 presents the asset pricing results for all models considered, with Panel A showing the specifications in (A1) and Panel B the frameworks in (A2). The results in Panel A indicate that none of the SDF loadings and risk prices for benchmark risk factors are statistically significant at the 5% confidence level. In contrast, we document the positive and statistically significant loading (a t-stat of 2.82) and price of the network risk factor (a t-stat of 2.67). In particular, the GMM estimate of $\lambda_{\mathcal{N}(S)}$ is 0.40% per month. Since the network

factor is actually tradable, we can apply the Euler equation to the factor excess returns and derive that its price of risk must be equal to the average excess return. Using statistics reported in Table A1 in Appendix, we verify that this no-arbitrage condition indeed holds: the monthly average return of 0.36% is close to the estimated price of 0.40%. Regarding the dollar factor, its SDF loading and price of risk are insignificant at conventional confidence levels (a t-stat of 1.25 for b_{dol} and a t-stat of 0.13 for λ_{dol}). Moreover, the estimated λ_{dol} matches the factor's average excess return of 0.01% per month, as reported in Table 4. Even though the dollar factor does not help to explain the average excess returns, it serves as a constant capturing the common mispricing in the cross-sectional regression.

In terms of the model fit, the two-factor SDFs combining the dollar and other benchmark risk factors produce similar performances, capturing from 25.31% to 40.21% of the total variance in the cross-sectional returns and yielding RMSEs from 0.11% to 0.12%. The HJ_{dist} distance values cannot be considered favorable to the SDFs based on the small p-values of around 0.05. At the same time, the SDF specification comprising the dollar and network risk factors outperforms other models by a large margin. For instance, it generates more than twice as large cross-sectional R^2 of 88.10% and around two times smaller RMSE and HJ_{dist} of 0.05% and 0.09. The simulated p-value of the HJ_{dist} distance indicates that we cannot reject this two-factor SDF at any conventional confidence level.

In sum, the benchmark risk factors from the existing literature have a hard time explaining the portfolios sorted on network connectedness, even though volatility linkages have strong contemporaneous correlations that serve as the proxy for common risks in currency returns. Meanwhile, the network risk factor successfully prices the novel cross-section of currency returns documented in our paper. Furthermore, the quantitative results show a significant wedge in the contribution of the network and other factors, despite possibly a common component in their returns originating from the interest rate predictability (for car), contemporaneous correlations in spot variances (for vol) or spot implied variances (for vrp).

Panel B in Table 15 shows the results for portfolios sorted on the net-directional connectedness controlling for contemporaneous correlations in volatility connections. As can be expected, once we eliminate the contemporaneous effects in the network, the performance

Table 15. Pricing Short-term Net-directional Network Portfolios: GMM Estimation

This table presents cross-sectional results. We price quintile portfolios ($\mathcal{P}_i : i = 1, \dots, 5$) sorted by short-term net-directional connectedness extracted from volatility linkages including (Panel A) or excluding (Panel B) contemporaneous correlations. The two-factor linear SDFs includes the dollar (dol) factor plus a second factor — carry trade (car), volatility (vol), volatility risk premium (vrp), momentum (mom), or short-term net-directional network ($\mathcal{N}(S)$) factor. The three-factor linear SDFs includes dol, $\mathcal{N}(S)$ plus a third factor — car, vol, vrp, or mom. Each panel reports one-step GMM estimates of factor loadings (b) and prices of factor risks (λ). Goodness-of-fit statistics include the R^2 and root mean squared pricing error (RMSE) (both are expressed in percentage), and the Hansen and Jagannathan (1997) distance (HJ_{dist}) with simulated p-values in parentheses. The p-values are for the null hypothesis that pricing errors are equal to zero. The remaining numbers in rows with a grey font are t-statistics of estimates, which are based on Newey and West (1987) standard errors. The sample is from January 1996 to January 2023.

	SDF loadings		Risk prices		Model fit				
	b_{dol}	b_{f_2}	λ_{dol}	λ_{f_2}	R^2 (%)	RMSE (%)	HJ_{dist}		
Panel A: Including contemporaneous correlations									
dol + car	-0.03	0.07	0.01	0.68	29.45	0.12	0.16		
	-0.81	1.42	0.07	1.42			0.06		
dol + vol	-0.17	0.24	0.01	1.26	39.08	0.11	0.15		
	-1.37	1.39	0.06	1.37			0.05		
dol + vrp	0.03	0.17	0.01	1.15	40.21	0.11	0.16		
	0.90	1.51	0.09	1.51			0.05		
dol + mom	0.04	0.26	0.00	1.79	25.31	0.12	0.17		
	0.88	1.47	-0.01	1.47			0.04		
dol + $\mathcal{N}(S)$	0.04	0.09	0.02	0.40	88.10	0.05	0.09		
	1.25	2.82	0.13	2.67			0.53		
Panel B: Excluding contemporaneous correlations									
dol + car	0.00	0.00	0.00	-0.03	0.13	0.15	0.24		
	0.00	-0.05	-0.04	-0.05			0.00		
dol + vol	0.00	-0.01	0.00	-0.03	0.12	0.15	0.25		
	0.03	-0.04	-0.04	-0.05			0.00		
dol + vrp	0.05	0.28	0.00	1.94	32.01	0.13	0.19		
	0.99	1.42	0.02	1.42			0.01		
dol + mom	0.06	0.36	0.01	2.50	37.31	0.12	0.22		
	0.99	1.25	0.05	1.25			0.00		
dol + $\mathcal{N}(S)$	0.02	0.06	0.00	0.31	45.31	0.11	0.18		
	0.64	2.46	0.03	2.43			0.01		
Panel C: Three-factor linear SDFs									
	SDF loadings			Risk prices			Model fit		
	b_{dol}	b_{f_2}	$b_{\mathcal{N}(S)}$	λ_{dol}	λ_{f_2}	$\lambda_{\mathcal{N}(S)}$	R^2 (%)	RMSE (%)	HJ_{dist}
dol + car + $\mathcal{N}(S)$	-0.05	0.20	0.13	0.01	1.74	0.41	99.30	0.01	0.02
	-1.12	2.46	3.35	0.05	2.32	2.30			0.95
dol + vol + $\mathcal{N}(S)$	-0.29	0.45	0.11	0.00	2.27	0.38	87.20	0.05	0.10
	-1.62	1.77	2.48	0.00	1.71	2.47			0.56
dol + vrp + $\mathcal{N}(S)$	0.07	0.24	0.07	0.03	1.66	0.40	80.01	0.07	0.11
	1.62	1.46	2.08	0.22	1.47	2.08			0.38
dol + mom + $\mathcal{N}(S)$	0.02	0.04	0.05	0.00	0.30	0.30	45.41	0.11	0.18
	0.53	0.15	2.34	0.04	0.17	2.26			0.00

of the SDFs with car and vol deteriorates significantly. The t-statistics of SDF loadings and factor prices become close to zero. Further, the R^2 statistics drop dramatically to 0.13% and 0.12% with car and vol as a second factor. Intuitively, the network connections exclude

Table 16. Pricing Short-term Net-directional Network Portfolios: Fama–MacBeth Estimation

This table presents cross-sectional results based on the two-stage procedure of Fama and MacBeth (1973). The test portfolios are quintile portfolios ($\mathcal{P}_i : i = 1, \dots, 5$) sorted by short-term net-directional connectedness extracted from volatility linkages including (Panel A) or excluding (Panel B) contemporaneous correlations. The two-factor models include the dollar (dol) factor plus a second factor — carry trade (car), volatility (vol), volatility risk premium (vrp), momentum (mom), or short-term net-directional network ($\mathcal{N}(S)$) factor. The three-factor models include dol, $\mathcal{N}(S)$ plus a third factor — car, vol, vrp, or mom. In the first stage, we estimate the time series regressions of test portfolios on a set of factors. In the second stage, we estimate the cross-sectional regression of average returns on the slope coefficients. We exclude the intercept in the second stage, consistent with the GMM estimation. Each panel reports estimates of prices of factor risks (λ) and their t-statistics based on Shanken (1992) standard errors. Goodness-of-fit statistics include the R^2 , χ^2 test statistic and associated p-value for the test that pricing errors are jointly equal to zero. The sample is from January 1996 to January 2023.

	Risk prices		Model fit			
	λ_{dol}	λ_{f_2}	R^2 (%)	χ^2	p-value	
Panel A: Including contemporaneous correlations						
dol + car	0.01	0.67	27.99	8.89	0.03	
	0.08	1.80				
dol + vol	0.01	1.25	37.19	7.98	0.05	
	0.06	1.86				
dol + vrp	0.01	1.15	38.80	8.20	0.04	
	0.10	2.11				
dol + mom	0.00	1.77	23.03	9.33	0.03	
	-0.01	1.53				
dol + $\mathcal{N}(S)$	0.02	0.40	87.86	2.37	0.50	
	0.14	3.02				
Panel B: Excluding contemporaneous correlations						
dol + car	0.00	-0.03	-0.42	20.65	0.00	
	-0.04	-0.05				
dol + vol	0.00	-0.03	-0.42	21.16	0.00	
	-0.04	-0.04				
dol + vrp	0.00	1.92	30.75	12.80	0.01	
	0.03	1.89				
dol + mom	0.01	2.47	35.72	16.10	0.00	
	0.09	1.57				
dol + $\mathcal{N}(S)$	0.00	0.31	44.99	10.82	0.01	
	0.03	2.22				
	Risk prices			Model fit		
	λ_{dol}	λ_{f_2}	$\lambda_{\mathcal{N}(S)}$	R^2 (%)	χ^2	p-value
dol + car + $\mathcal{N}(S)$	0.01	1.74	0.41	99.30	0.18	0.92
	0.08	2.57	3.07			
dol + vol + $\mathcal{N}(S)$	0.00	2.27	0.38	87.01	3.49	0.17
	0.01	1.91	2.73			
dol + vrp + $\mathcal{N}(S)$	0.01	2.21	0.37	85.82	3.85	0.15
	0.12	2.10	2.73			
dol + mom + $\mathcal{N}(S)$	0.00	0.28	0.30	45.08	10.70	0.00
	0.04	0.16	2.21			

the common component in the risk-neutral volatilities on exchange rates and, as a result, the performance of the SDFs with car and vol deteriorates significantly. Interestingly, the performance of the two-factor linear model combining dol with vrp or mom does not de-

teriorate significantly or even improve, though there is no statistical evidence on priced volatility premium or momentum risk. In contrast, the factor loading and price of network risk is statistically significant at the 5% level (a t-stat of 2.46 for $b_{\mathcal{N}(S)}$ and a t-stat of 2.43 for $\lambda_{\mathcal{N}(S)}$). The model with the network factor also displays stronger explanatory power as measured by higher R^2 (45.31%) and generates lower pricing errors as measured by lower RMSE (0.11%) and HJ_{dist} (0.18). Nevertheless, none of these two-factor SDF specifications can explain the cross-sectional differences in average network returns based on the close-to-zero p-values of HJ_{dist} . Furthermore, the GMM estimate of $\lambda_{\mathcal{N}(S)}$ is 0.30% per month. Using statistics reported in Table 2, the monthly average return of 0.42% is above the estimated price of 0.30%. This violation of the no-arbitrage condition indicates that the proposed SDF may not fully explain the variation in test asset returns.

In Panel B in Table 15, we extend the two-factor model with dol and $\mathcal{N}(S)$ to the three-factor specification with car, vol, vrp or mom. The inclusion of an additional factor generally leads to a higher R^2 , lower RMSE and HJ_{dist} statistics relative to the original two-factor SDF. Most importantly, network risk remains strongly priced in all specifications. Consistent with the principal component decomposition, the best-performing three-factor model includes the dollar, carry trade, and network risk factors. In this case, the estimated price of risk of the network factor is 0.41%, close to the average monthly return of 0.42%. Moreover, the SDF specification is able to explain 99.30% of the cross-sectional variation in average network portfolio returns and cannot be rejected at any conventional confidence level due to the p-values of the (HJ_{dist}) distance of 0.95.

We now employ the standard Fama–MacBeth regression (Fama and MacBeth, 1973) to obtain the factor loadings and risk prices. We compare the results for short-term net-directional network portfolios with those implied by the GMM estimates. Table 16 presents the regression outputs. The results of the Fama–MacBeth procedure are qualitatively and quantitatively similar to those reported in Table 15.

In sum, the comparison of different estimation procedures reinforces the robustness of the key conclusion: the novel network-sorted cross-section of currency returns cannot be understood through the lens of common currency strategies. When volatility linkages include contemporaneous correlations, the network risk factor fully explains the cross-

sectional differences in average quintile returns, whereas common factors are not priced in the network cross-section. Surprisingly, when volatility linkages control for contemporaneous correlations, the network risk factor is not the only source of priced risk in the second cross-section of network-sorted returns. Instead, the combination of the carry trade and network portfolios is required to fully explain the currency returns. The economic mechanism behind this result looks as follows. We have removed the contemporaneous correlations between the volatility linkages that are used to construct the network portfolios. Although the network factor possesses the predictive power of volatility linkages between individual currencies, it does not contain the predictive information associated with the common time variation in all currency volatilities. The latter component can be captured by a global risk factor, which is typically associated with the carry trade strategy. As a result, the three-factor SDF with the dollar (common mispricing in currency returns), the carry trade (common fluctuations in exchange rates), and the network factor (asymmetric connections between currency volatilities) can explain the currency portfolios sorted on free-from-correlation network connectedness.

5.4 Time-series Exposure to Network Factors

We further estimate the sensitivity of excess returns of quintile portfolios ($\mathcal{P}_i : i = 1, \dots, 5$) to the network risk. Table 17 reports the outputs of a contemporaneous regression of excess returns of each quintile portfolio on the dollar and network risk factors (Panel A) and on the dollar, network risk factor, and one of the remaining benchmarks (Panel B).

For currency returns sorted on network connections with contemporaneous effects, the alphas are statistically insignificant. The β_{dol} coefficients are close one. The β_{net} coefficients display pronounced monotonicity when we move from \mathcal{P}_1 to \mathcal{P}_5 , increasing from -0.44 (a t-stat of -20.33) to 0.56 (a t-stat of 25.74). The two factors capture a lot of variation of quintile portfolios ranging from 68.41% for \mathcal{P}_4 to 93.25% for \mathcal{P}_1 .

For currency returns sorted on free-from-correlation network connections, the right part of Panels A and Panel B reports the outputs for two- and three-factor regressions. The results suggest that the first and fifth quintiles have statistically significant alphas at the 1% confidence level when we include vol, vrp, or mom. In contrast, the inclusion of the carry trade substantially reduces the magnitude of alphas of the lowest and highest network

Table 17. Net-directional Network Portfolios: Factor Betas

This table presents a contemporaneous regression of monthly excess returns of each quintile portfolio on two risk factors — the dollar and short-term net-directional network portfolios (Panel A), or on three risk factors — the dollar, a short-term net-directional network portfolio plus a third factor, including car, vol, vrp, or mom (Panel B). Constants reported in the “alpha” row are expressed in percentage per annum. The numbers in rows with a grey font are t-statistics of estimates, which are based on [Newey and West \(1987\)](#) standard errors. The last row in each panel shows the adjusted R^2 (in percentage). The sample is from January 1996 to January 2023.

Panel A: Short-term net-directional portfolios										
	Inc. contemporaneous correlations					Exc. contemporaneous correlations				
	\mathcal{P}_1	\mathcal{P}_2	\mathcal{P}_3	\mathcal{P}_4	\mathcal{P}_5	\mathcal{P}_1	\mathcal{P}_2	\mathcal{P}_3	\mathcal{P}_4	\mathcal{P}_5
alpha (% , annual)	0.46	-0.38	-0.84	0.74	0.46	1.75	-0.78	-1.27	-1.38	1.75
	0.96	-0.55	-0.95	0.78	0.96	3.33	-1.10	-1.93	-1.82	3.33
β_{dol}	1.01	1.09	0.99	0.91	1.01	0.90	1.14	1.09	0.97	0.90
	44.34	25.77	31.24	25.87	44.34	35.10	30.90	38.84	30.71	35.10
$\beta_{N(s)}$	-0.44	-0.19	-0.02	0.10	0.56	-0.63	0.00	0.07	0.16	0.37
	-20.33	-6.28	-0.66	2.72	25.74	-17.87	-0.01	2.39	5.73	10.64
$R^2(\%)$	93.25	89.07	76.70	68.41	88.85	92.62	84.85	86.30	78.64	85.71
Panel B: Short-term net-directional portfolios: excluding contemporaneous correlations										
	car					vol				
	\mathcal{P}_1	\mathcal{P}_2	\mathcal{P}_3	\mathcal{P}_4	\mathcal{P}_5	\mathcal{P}_1	\mathcal{P}_2	\mathcal{P}_3	\mathcal{P}_4	\mathcal{P}_5
alpha (% , annual)	1.22	-0.48	-0.92	-1.04	1.22	1.58	-0.62	-1.22	-1.35	1.58
	2.19	-0.64	-1.34	-1.25	2.19	3.16	-0.88	-1.81	-1.68	3.16
β_{dol}	0.87	1.16	1.11	0.99	0.87	0.86	1.18	1.10	0.98	0.86
	31.60	29.61	40.43	35.69	31.60	26.40	26.99	34.86	26.93	26.40
β_{f_2}	0.08	-0.05	-0.05	-0.05	0.08	0.06	-0.06	-0.02	-0.01	0.06
	4.09	-1.70	-2.18	-1.96	4.09	1.90	-1.46	-0.63	-0.33	1.90
$\beta_{N(s)}$	-0.61	-0.01	0.06	0.15	0.39	-0.62	-0.01	0.07	0.16	0.38
	-20.15	-0.33	2.00	4.95	13.06	-18.80	-0.15	2.31	5.40	11.44
$R^2(\%)$	93.58	85.36	86.94	79.31	87.24	93.09	85.31	86.60	78.90	86.31
	vrp					mom				
	\mathcal{P}_1	\mathcal{P}_2	\mathcal{P}_3	\mathcal{P}_4	\mathcal{P}_5	\mathcal{P}_1	\mathcal{P}_2	\mathcal{P}_3	\mathcal{P}_4	\mathcal{P}_5
alpha (% , annual)	1.70	-0.73	-1.25	-1.36	1.70	1.74	-0.71	-1.26	-1.43	1.74
	3.22	-1.04	-1.87	-1.78	3.22	3.24	-0.98	-1.94	-1.92	3.24
β_{dol}	0.90	1.13	1.09	0.97	0.90	0.90	1.14	1.09	0.98	0.90
	38.87	33.25	38.76	28.57	38.87	34.86	29.65	38.00	32.02	34.86
β_{f_2}	0.05	-0.07	-0.02	-0.02	0.05	0.00	-0.03	0.00	0.02	0.00
	1.74	-1.89	-0.72	-0.54	1.74	0.03	-1.11	-0.18	0.97	0.03
$\beta_{N(s)}$	-0.63	0.00	0.08	0.16	0.37	-0.63	0.00	0.08	0.16	0.37
	-18.94	0.03	2.47	5.83	11.23	-17.69	0.09	2.35	5.58	10.53
$R^2(\%)$	93.11	85.49	86.62	78.93	86.36	92.90	85.22	86.58	78.95	85.98

characteristic quintiles, which become significant at the 5% confidence level now. This can be explained by the observation that the exposure to the carry trade factor is statistically significant, while the beta estimates for the other factors are generally insignificant for three excess returns. The goodness of fit and slope coefficients of the network risk factor remains largely unchanged for two- and three-factor regressions.

Overall, the results of time-series regressions are consistent with cross-sectional regressions. Specifically, they reinforce the conclusion that the dollar and network risk factors fully explain the sources of risk in the cross-section formed on network connectedness measures with common fluctuations, while the dollar, carry trade, and network factors explain the cross-section based on network connectedness controlling for common fluctuations.

6 Conclusion

We estimate dynamically changing connections among option-implied volatilities on exchange rates and demonstrate that the structure in volatility linkages predicts currency returns. The currency network strategy, which buys net recipients and sells net transmitters of transitory volatility shocks, generates a high Sharpe ratio and yields a significant alpha when controlling for popular foreign exchange benchmarks. Trading currency connectedness at longer horizons is less profitable, indicating a downward-sloping term structure of volatility network risk in currency markets. The cross-sectional variation of network-sorted excess returns cannot be understood through the lens of existing risk factors — dollar, carry trade, volatility, volatility risk premium, and momentum. Interestingly, the combination of the dollar, carry trade, and network risk factors fully explain the excess returns formed on network risk measures controlling for contemporaneous effects. In robustness checks, we show that the performance of network portfolios in terms of risk-adjusted (Sharpe ratios) and benchmark-adjusted (estimated alphas) performances actually improves when the strategies are implemented at the weekly frequency. The significance of monthly network excess returns is also robust to transaction costs, subperiods, and usage of option-implied variances. Finally, the predictive power of the network connectedness measures disappears when we employ the realized currency volatilities. This emphasizes a critical contribution of the forward-looking information contained in option-implied volatilities.

Overall, we provide new insights into the sources of currency predictability. While our findings are economically intuitive and complement the existing evidence on the global volatility risk factor in foreign exchange markets, our understanding of currency volatility spillovers requires further work. Motivated by the evidence in this paper, developing a macro-finance framework linking volatility linkages to currency excess returns is a promising avenue for future research.

References

- Akram, Q. F., D. Rime, and L. Sarno (2008). Arbitrage in the foreign exchange market: Turning on the microscope. *Journal of International Economics* 76(2), 237–253.
- Andersen, L., D. Duffie, and Y. Song (2019). Funding value adjustments. *The Journal of Finance* 74(1), 145–192.
- Asness, C. S., T. J. Moskowitz, and L. H. Pedersen (2013). Value and momentum everywhere. *The Journal of Finance* 68(3), 929–985.
- Bakshi, G., N. Kapadia, and D. Madan (2003). Stock return characteristics, skew laws, and the differential pricing of individual equity options. *The Review of Financial Studies* 16(1), 101–143.
- Bakshi, G. and G. Panayotov (2013). Predictability of currency carry trades and asset pricing implications. *Journal of financial economics* 110(1), 139–163.
- Bansal, R. and A. Yaron (2004). Risks for the long run: A potential resolution of asset pricing puzzles. *The Journal of Finance* 59 (4), 1481–1509.
- Barunik, J. and M. Ellington (2020). Dynamic networks in large financial and economic systems. *arXiv preprint arXiv:2007.07842*.
- BIS (2019a). Otc derivatives statistics at end-june 2019. *Bank for International Settlements, Basel*.
- BIS (2019b). Triennial central bank survey of foreign exchange and otc derivatives markets activity in 2019. *Bank for International Settlements, Basel*.
- Britten-Jones, M. and A. Neuberger (2000). Option prices, implied price processes, and stochastic volatility. *Journal of Finance* 55, 839–866.
- Burnside, C., M. Eichenbaum, I. Kleshchelski, and S. Rebelo (2011). Do peso problems explain the returns to the carry trade? *The Review of Financial Studies* 24(3), 853–891.
- Campa, J. M. and P. K. Chang (1995). Testing the expectations hypothesis on the term structure of volatilities in foreign exchange options. *The Journal of finance* 50(2), 529–547.
- Cespa, G., A. Gargano, S. J. Riddiough, and L. Sarno (2021, 09). Foreign exchange volume. *The Review of Financial Studies*.
- Chernov, M., J. Graveline, and I. Zviadadze (2018). Crash risk in currency returns. *Journal of Financial and Quantitative Analysis* 53(1), 137–170.
- Cochrane, J. H. (2005). *Asset pricing*. Princeton university press.

- Colacito, R., M. M. Croce, F. Gavazzoni, and R. Ready (2018). Currency risk factors in a recursive multicountry economy. *The Journal of Finance* 73(6), 2719–2756.
- Colacito, R., S. J. Riddiough, and L. Sarno (2020). Business cycles and currency returns. *Journal of Financial Economics*.
- Corte, P. D., S. J. Riddiough, and L. Sarno (2016). Currency premia and global imbalances. *The Review of Financial Studies* 29(8), 2161–2193.
- Dahlhaus, R. (1996). On the kullback-leibler information divergence of locally stationary processes. *Stochastic processes and their applications* 62(1), 139–168.
- Dahlhaus, R., W. Polonik, et al. (2009). Empirical spectral processes for locally stationary time series. *Bernoulli* 15(1), 1–39.
- Dahlquist, M. and H. Hasseltoft (2020). Economic momentum and currency returns. *Journal of Financial Economics* 136(1), 152–167.
- Della Corte, P., R. Kozhan, and A. Neuberger (2021). The cross-section of currency volatility premia. *Journal of Financial Economics* 139(3), 950–970.
- Della Corte, P., R. Kozhan, and A. Neuberger (2022). Arbitrage bounds on cross currency options. Available at SSRN 4293500.
- Della Corte, P., T. Ramadorai, and L. Sarno (2016). Volatility risk premia and exchange rate predictability. *Journal of Financial Economics* 120(1), 21–40.
- Dew-Becker, I., S. Giglio, A. Le, and M. Rodriguez (2017). The price of variance risk. *Journal of Financial Economics* 123(2), 225–250.
- Diebold, F. X. and K. Yilmaz (2014). On the network topology of variance decompositions: Measuring the connectedness of financial firms. *Journal of Econometrics* 182(1), 119–134.
- Du, W., A. Tepper, and A. Verdelhan (2018). Deviations from covered interest rate parity. *The Journal of Finance* 73(3), 915–957.
- Eraker, B. and Y. Wu (2017). Explaining the negative returns to volatility claims: An equilibrium approach. *Journal of Financial Economics* 125(1), 72–98.
- Fama, E. F. and K. R. French (1993). Common risk factors in the returns on stocks and bonds. *Journal of financial economics* 33(1), 3–56.
- Fama, E. F. and J. D. MacBeth (1973). Risk, return, and equilibrium: Empirical tests. *Journal of political economy* 81(3), 607–636.
- Fan, Z., J. M. Londono, and X. Xiao (2021). Equity tail risk and currency risk premiums.

Journal of Financial Economics.

- Farhi, E., S. P. Fraiberger, X. Gabaix, R. Ranciere, and A. Verdelhan (2015). Crash risk in currency markets. Technical report, New York University, New York, NY.
- Fung, W. and D. A. Hsieh (2004). Hedge fund benchmarks: A risk-based approach. *Financial Analysts Journal* 60(5), 65–80.
- Gabaix, X. and M. Maggiori (2015). International liquidity and exchange rate dynamics. *The Quarterly Journal of Economics* 130(3), 1369–1420.
- Garman, M. B. and S. W. Kohlhagen (1983). Foreign currency option values. *Journal of International Money and Finance* 2(3), 231–237.
- Gilmore, S. and F. Hayashi (2011). Emerging market currency excess returns. *American Economic Journal: Macroeconomics* 3(4), 85–111.
- Goyal, A. and A. Saretto (2009). Cross-section of option returns and volatility. *Journal of Financial Economics* 94(2), 310–326.
- Hansen, L. P. (1982). Large sample properties of generalized method of moments estimators. *Econometrica: Journal of the Econometric Society*, 1029–1054.
- Hansen, L. P. and R. Jagannathan (1997). Assessing specification errors in stochastic discount factor models. *The Journal of Finance* 52(2), 557–590.
- Herskovic, B., B. Kelly, H. Lustig, and S. Van Nieuwerburgh (2020). Firm volatility in granular networks. *Journal of Political Economy* 128(11), 4097–4162.
- Jagannathan, R. and Z. Wang (1996). The conditional capm and the cross-section of expected returns. *The Journal of Finance* 51(1), 3–53.
- Johnson, T. L. (2017). Risk premia and the vix term structure. *Journal of Financial and Quantitative Analysis* 52(6), 2461–2490.
- Jurek, J. W. (2014). Crash-neutral currency carry trades. *Journal of Financial Economics* 113(3), 325–347.
- Kadiyala, K. R. and S. Karlsson (1997). Numerical methods for estimation and inference in Bayesian VAR-models. *Journal of Applied Econometrics* 12(2), 99–132.
- Kan, R. and C. Robotti (2008). Specification tests of asset pricing models using excess returns. *Journal of Empirical Finance* 15(5), 816–838.
- Londono, J. M. and H. Zhou (2017). Variance risk premiums and the forward premium puzzle. *Journal of Financial Economics* 124(2), 415–440.

- Lustig, H., N. Roussanov, and A. Verdelhan (2011). Common risk factors in currency markets. *The Review of Financial Studies* 24(11), 3731–3777.
- Lustig, H. and A. Verdelhan (2007). The cross section of foreign currency risk premia and consumption growth risk. *American Economic Review* 97(1), 89–117.
- Lütkepohl, H. (2005). *New introduction to multiple time series analysis*. Springer Science & Business Media.
- Lyons, R. K. et al. (2001). *The microstructure approach to exchange rates*, Volume 333. Citeseer.
- Menkhoff, L., L. Sarno, M. Schmeling, and A. Schrimpf (2012a). Carry trades and global foreign exchange volatility. *The Journal of Finance* 67(2), 681–718.
- Menkhoff, L., L. Sarno, M. Schmeling, and A. Schrimpf (2012b). Currency momentum strategies. *Journal of Financial Economics* 106(3), 660–684.
- Menkhoff, L., L. Sarno, M. Schmeling, and A. Schrimpf (2017). Currency value. *The Review of Financial Studies* 30(2), 416–441.
- Mueller, P., A. Stathopoulos, and A. Vedolin (2017). International correlation risk. *Journal of Financial Economics* 126(2), 270–299.
- Newey, W. and K. West (1987). A simple, positive semi-definite, heteroskedasticity and autocorrelation consistent covariance matrix. *Econometrica*, 703–708.
- Pástor, L. and R. F. Stambaugh (2003). Liquidity risk and expected stock returns. *Journal of Political economy* 111(3), 642–685.
- Pesaran, H. H. and Y. Shin (1998). Generalized impulse response analysis in linear multivariate models. *Economics letters* 58(1), 17–29.
- Petrova, K. (2019). A quasi-Bayesian local likelihood approach to time varying parameter VAR models. *Journal of Econometrics*.
- Richmond, R. J. (2019). Trade network centrality and currency risk premia. *The Journal of Finance* 74(3), 1315–1361.
- Shanken, J. (1992). On the estimation of beta-pricing models. *The review of financial studies* 5(1), 1–33.
- Zviadadze, I. (2017). Term structure of consumption risk premia in the cross section of currency returns. *The Journal of Finance* 72(4), 1529–1566.

Appendix for

“Currency Network Risk”

Abstract

This appendix presents supplementary details not included in the main body of the paper.

A Estimation of the time-varying parameter VAR model

Let \mathbf{CIV}_t be an $N \times 1$ vector generated by a stable time-varying parameter (TVP) heteroskedastic VAR model with p lags:

$$\mathbf{CIV}_{t,T} = \Phi_1(t/T)\mathbf{CIV}_{t-1,T} + \dots + \Phi_p(t/T)\mathbf{CIV}_{t-p,T} + \epsilon_{t,T}, \quad (\text{A.1})$$

where $\epsilon_{t,T} = \Sigma^{-1/2}(t/T)\eta_{t,T}$, $\eta_{t,T} \sim NID(0, \mathbf{I}_M)$ and $\Phi(t/T) = (\Phi_1(t/T), \dots, \Phi_p(t/T))^\top$ are the time-varying autoregressive coefficients. Note that all roots of the polynomial $\chi(z) = \det(\mathbf{I}_N - \sum_{p=1}^L z^p \mathbf{B}_{p,t})$ lie outside the unit circle, and Σ_t^{-1} is a positive definite time-varying covariance matrix. Stacking the time-varying intercepts and autoregressive matrices in the vector $\phi_{t,T}$ with $\overline{\mathbf{CIV}}_t^\top = (\mathbf{I}_N \otimes x_t)$, $x_t = (1, x_{t-1}^\top, \dots, x_{t-p}^\top)$ and denoting the Kronecker product by \otimes , the model can be written as:

$$\mathbf{CIV}_{t,T} = \overline{\mathbf{CIV}}_{t,T}^\top \phi_{t,T} + \Sigma_{t/T}^{-\frac{1}{2}} \eta_{t,T} \quad (\text{A.2})$$

We obtain the time-varying parameters of the model by employing the Quasi-Bayesian Local-Likelihood (QBLL) approach of Petrova (2019). The estimation of Eq. (A.1) requires re-weighting the likelihood function. The weighting function gives higher proportions to observations surrounding the time period whose parameter values are of interest. The local likelihood function at time period k is given by:

$$\begin{aligned} & L_k(\mathbf{CIV} | \theta_k, \Sigma_k, \overline{\mathbf{CIV}}) \propto \\ & |\Sigma_k|^{\text{trace}(\mathbf{D}_k)/2} \exp \left\{ -\frac{1}{2} (\mathbf{CIV} - \overline{\mathbf{CIV}}^\top \phi_k)^\top (\Sigma_k \otimes \mathbf{D}_k) (\mathbf{CIV} - \overline{\mathbf{CIV}}^\top \phi_k) \right\} \end{aligned} \quad (\text{A.3})$$

\mathbf{D}_k is a diagonal matrix whose elements hold the weights:

$$\mathbf{D}_k = \text{diag}(q_{k1}, \dots, q_{kT}) \quad (\text{A.4})$$

$$q_{kt} = \phi_{T,k} w_{kt} / \sum_{t=1}^T w_{kt} \quad (\text{A.5})$$

$$w_{kt} = (1/\sqrt{2\pi}) \exp((-1/2)((k-t)/H)^2), \quad \text{for } k, t \in \{1, \dots, T\} \quad (\text{A.6})$$

$$\zeta_{Tk} = \left(\left(\sum_{t=1}^T w_{kt} \right)^2 \right)^{-1} \quad (\text{A.7})$$

where q_{kt} is a normalised kernel function. w_{kt} uses a Normal kernel weighting function. ζ_{Tk} gives the rate of convergence and behaves like the bandwidth parameter H in (A.6). The kernel function puts a greater weight on the observations surrounding the parameter estimates at time k relative to more distant observations.

We use a Normal-Wishart prior distribution for $\phi_k | \Sigma_k$ for $k \in \{1, \dots, T\}$:

$$\phi_k | \Sigma_k \sim \mathcal{N} \left(\phi_{0k}, (\Sigma_k \otimes \Xi_{0k})^{-1} \right) \quad (\text{A.8})$$

$$\Sigma_k \sim \mathcal{W}(\alpha_{0k}, \Gamma_{0k}) \quad (\text{A.9})$$

where ϕ_{0k} is a vector of prior means, Ξ_{0k} is a positive definite matrix, α_{0k} is a scale parameter of the Wishart distribution (\mathcal{W}), and Γ_{0k} is a positive definite matrix.

The prior and weighted likelihood function implies a Normal-Wishart quasi posterior distribution for $\phi_k | \Sigma_k$ for $k = \{1, \dots, T\}$. Formally, let $\mathbf{A} = (\bar{x}_1^\top, \dots, \bar{x}_T^\top)^\top$ and $\mathbf{Y} = (x_1, \dots, x_T)^\top$, then:

$$\phi_k | \Sigma_k, \mathbf{A}, \mathbf{Y} \sim \mathcal{N} \left(\tilde{\theta}_k, (\Sigma_k \otimes \tilde{\Xi}_k)^{-1} \right) \quad (\text{A.10})$$

$$\Sigma_k \sim \mathcal{W}(\tilde{\alpha}_k, \tilde{\Gamma}_k^{-1}) \quad (\text{A.11})$$

with quasi-posterior parameters

$$\tilde{\phi}_k = \left(\mathbf{I}_N \otimes \tilde{\Xi}_k^{-1} \right) \left[\left(\mathbf{I}_N \otimes \mathbf{A}^\top \mathbf{D}_k \mathbf{A} \right) \hat{\phi}_k + \left(\mathbf{I}_N \otimes \Xi_{0k} \right) \phi_{0k} \right] \quad (\text{A.12})$$

$$\tilde{\Xi}_k = \tilde{\Xi}_{0k} + \mathbf{A}^\top \mathbf{D}_k \mathbf{A} \quad (\text{A.13})$$

$$\tilde{\alpha}_k = \alpha_{0k} + \sum_{t=1}^T q_{kt} \quad (\text{A.14})$$

$$\tilde{\Gamma}_k = \Gamma_{0k} + \mathbf{Y}' \mathbf{D}_k \mathbf{Y} + \Phi_{0k} \Gamma_{0k} \Phi_{0k}^\top - \tilde{\Phi}_k \tilde{\Gamma}_k \tilde{\Phi}_k^\top \quad (\text{A.15})$$

where $\hat{\phi}_k = (\mathbf{I}_N \otimes \mathbf{A}^\top \mathbf{D}_k \mathbf{A})^{-1} (\mathbf{I}_N \otimes \mathbf{A}^\top \mathbf{D}_k) y$ is the local likelihood estimator for ϕ_k . The matrices Φ_{0k} , $\tilde{\Phi}_k$ are conformable matrices from the vector of prior means, ϕ_{0k} , and a draw from the quasi posterior distribution, $\tilde{\phi}_k$, respectively.

The motivation for employing these methods is threefold. First, we are able to estimate large systems that conventional Bayesian estimation methods do not permit. This is typical

because the state-space representation of an N -dimensional TVP VAR (p) requires an additional $N(3/2 + N(p + 1/2))$ state equations for every additional variable. Conventional Markov Chain Monte Carlo (MCMC) methods fail to estimate larger models, which in general confine one to (usually) fewer than 6 variables in the system. Second, the standard approach is fully parametric and requires a law of motion. This can distort inference if the true law of motion is misspecified. Third, the methods used here permit direct estimation of the VAR's time-varying covariance matrix, which has an inverse-Wishart density and is symmetric positive definite at every point in time.

In estimating the model, we use $p=2$ and a Minnesota Normal-Wishart prior with a shrinkage value $\varphi = 0.05$ and centre the coefficient on the first lag of each variable to 0.1 in each respective equation. The prior for the Wishart parameters are set following [Kadiyala and Karlsson \(1997\)](#). For each point in time, we run 500 simulations of the model to generate the (quasi) posterior distribution of parameter estimates. Note we experiment with various lag lengths, $p = \{2, 3, 4, 5\}$; shrinkage values, $\varphi = \{0.01, 0.25, 0.5\}$; and values to centre the coefficient on the first lag of each variable, $\{0, 0.05, 0.2, 0.5\}$. Network measures from these experiments are qualitatively similar. Notably, adding lags to the VAR and increasing the persistence in the prior value of the first lagged dependent variable in each equation increases computation time.

Finally, the variance decompositions of forecast errors from the VMA(∞) representation require truncation of the infinite horizon with a H horizon approximation. As $H \rightarrow \infty$ the error disappears ([Lütkepohl, 2005](#)). We note here that H serves as an approximating factor and has no interpretation in the time domain. We obtain horizon-specific measures using Fourier transforms and set our truncation horizon $H=100$. The results are qualitatively similar for $H \in \{50, 100, 200\}$.

B Asset Pricing Tests

The Euler equation implies that the excess returns rx_{t+1}^j of a portfolio j satisfy the equation:

$$\mathbb{E}_t \left(M_{t+1} rx_{t+1}^j \right) = 0, \quad (\text{B.16})$$

in which M_{t+1} is the stochastic discount factor (SDF). We assume that the SDF is a linear function of a set of risk factors f_{t+1} and is defined as follows:

$$M_{t+1} = 1 - b'(f_{t+1} - \mu_f). \quad (\text{B.17})$$

Notice that we employ a de-meanned version of the SDF to avoid the issue related to an affine transformation of factors (Kan and Robotti, 2008).

We are interested in testing the performance of linear pricing models defined by Eq. (B.16)-(B.17). To do so, we estimate factor loadings using the generalized method of moments (GMM) (Hansen, 1982). Substituting Eq. (B.17) into Eq. (B.16), we obtain the following N moment conditions $\mathbb{E}_t([1 - b'(f_{t+1} - \mu_f)]rx_{t+1}) = 0_N$, where rx_{t+1} is the N -dimensional vector of test asset excess returns. We simultaneously estimate the unknown vector of factor means μ_f . Thus, GMM moment conditions also include the set of k restrictions $\mathbb{E}_t(f_{t+1} - \mu_f) = 0_k$, where k denotes the number of factors in the SDF specification. Therefore, we have the following population moment conditions:

$$\mathbb{E}_t[g_{t+1}(\theta)] = \mathbb{E}_t \begin{bmatrix} [1 - b'(f_{t+1} - \mu_f)]rx_{t+1} \\ f_{t+1} - \mu_f \end{bmatrix} = 0_{N+k},$$

where $\theta = (b', \mu_f)'$ is the vector of parameters. The sample moment conditions are then defined as:

$$\bar{g}_T(\theta) = \begin{bmatrix} \bar{g}_T^1(\theta) \\ \bar{g}_T^2(\theta) \end{bmatrix} = \begin{bmatrix} \frac{1}{T} \sum_{t=1}^T [1 - b'(f_{t+1} - \mu_f)] rx_{t+1} \\ \frac{1}{T} \sum_{t=1}^T [f_{t+1} - \mu_f] \end{bmatrix}.$$

We implement a one-stage GMM estimation with the prespecified weighting matrix consisting of the identity matrix I_N for the first moment conditions and a large weight assigned to the remaining restrictions. Standard errors are computed based on a heteroscedasticity and autocorrelation consistent (HAC) estimate of the long-run covariance matrix $S = \sum_{j=-\infty}^{\infty} \mathbb{E}[g(\theta)g(\theta)']$ by the Newey and West (1987) procedure.

We now evaluate the performance of linear pricing models in explaining the cross-section of network portfolios. We construct the cross-sectional R^2 , root mean squared pricing error (RMSE), and the Hansen and Jagannathan (1997) distance (HJ_{dist}). Hansen

and Jagannathan (1997) provide two nice illustrations of HJ_{dist} . First, it is the maximum pricing error of a portfolio with a unit second moment. Second, it measures the minimum distance between the proposed SDF and the set of admissible SDFs. Thus, tests of linear SDFs defined by Eq. (B.17) boil down to testing the null hypothesis that the pricing errors equal zero, i.e. HJ_{dist} equals zero. Formally, the Hansen and Jagannathan (1997) distance is defined as:

$$HJ_{\text{dist}} = \sqrt{\min_{\theta} \bar{g}_T(\theta)' G_T^{-1} \bar{g}_T(\theta)}, \quad (\text{B.18})$$

in which G_T is the sample second moment matrix of test excess returns, that is, $G_T = \frac{1}{T} \sum_{t=1}^T rx_{t+1}rx'_{t+1}$. One can obtain HJ_{dist} by applying the one-stage GMM estimation with the weighting matrix equal to G_T^{-1} . The advantage of this definition is that G_T^{-1} is independent of optimal parameters and hence this allows the comparison between different SDF specifications (Hansen and Jagannathan, 1997). The disadvantage of this approach is that G_T^{-1} is not optimal in the sense of Hansen (1982) and hence HJ_{dist} is not asymptotically a random variable of $\chi^2(N - k)$ distribution. Instead, the sample HJ_{dist} follows a weighted sum of $\chi^2(1)$ random variables (see Jagannathan and Wang (1996) and Kan and Robotti (2008) for specification tests using gross and excess returns, respectively). Therefore, we calculate the simulated p-values for HJ_{dist} based on this statistic.

C Transaction Costs

We use time-varying quoted bid-ask spreads to compute the currency excess returns adjusted for transaction costs. Following Menkhoff, Sarno, Schmeling, and Schrimpf (2012b), we take into account the whole cycle of each currency in the short or long positions from $t - 1$ to $t + 1$. When the investor buys the currency at time t and sells at time $t + 1$, he pays the corresponding bid-ask costs each period. In our notations, the excess returns of long (l) and short (s) positions are respectively $rx_{t+1}^l = f_t^b - s_{t+1}^a$ and $rx_{t+1}^s = -f_t^a + s_{t+1}^b$. If the investor buys the currency at time t but decides to keep it in the portfolio at time $t + 1$, then the net excess returns are computed as $rx_{t+1}^l = f_t^b - s_{t+1}$ and $rx_{t+1}^s = -f_t^a + s_{t+1}$. If the currency, which belongs to the portfolio at time t and is sold at time $t + 1$, was already in the current portfolio at time $t - 1$, then the excess returns $rx_{t+1}^l = f_t^b - s_{t+1}^a$ and $rx_{t+1}^s = -f_t^a + s_{t+1}^b$, that is, the investor must still initiate a position in the one-month for-

ward contract. At the start (January 1996) and at the end (December 2013) of the sample, the investor is assumed to start and close positions in all foreign currencies.

D Additional Results

We also examine the currency portfolios formed on network connectedness measures including contemporaneous correlations between volatility shocks. Table A1 reports summary statistics of net-directional network portfolios and shows that they produce similar patterns as the corresponding portfolios formed on free-from-correlation connectedness measures. Table A2 presents the correlations of net-directional network portfolios with standard currency strategies and regression outputs when controlling for common risk factors. The returns of a network portfolio formed on transitory volatility shocks are partially subsumed by the dollar and carry trade factors, however, they remain economically and statistically significant. It is worth noting that the network strategies that do not control for contemporaneous effects exhibit a positive and strong correlation with carry trade, especially those formed on more persistent volatility linkages. Table A3 shows that this generates smaller diversification gains. Table A4 further demonstrates that the performance of the net-directional network portfolio deteriorates after the 2007-2008 financial crisis, similar to common currency strategies. Table A5 reports an allocation analysis for quintile portfolios sorted by short-term net-directional connectedness based on volatility linkages excluding or including contemporaneous correlations. Table A6 presents summary statistics of a contemporaneous regression of monthly returns of a short-term net-directional strategy ($\mathcal{N}(S)$) on the equity and hedge fund strategies.

Table A1. Net-directional Network Portfolios: Including Contemporaneous Correlations

This table presents descriptive statistics for quintile ($\mathcal{P}_i : i = 1, \dots, 5$) and long-short portfolios ($\mathcal{N}(\cdot)$) sorted by short- (S), medium- (M), and long-term (L) as well as total (T) net-directional connectedness based on volatility linkages including contemporaneous correlations. The portfolio $\mathcal{P}_1(\mathcal{P}_5)$ comprises currencies with the highest (lowest) network characteristic. The long-short portfolio buys \mathcal{P}_5 and sells \mathcal{P}_1 . Mean, standard deviation, and Sharpe ratio are annualized, but the t-statistic of mean, skewness, kurtosis, and the first-order autocorrelation are based on monthly returns. We also report the annualized mean of the exchange rate ($fx = -\Delta s^k$) and interest rate ($ir = i^k - i$) components of excess returns. The t-statistics are based on [Newey and West \(1987\)](#) standard errors. The sample is from January 1996 to January 2023.

	\mathcal{P}_1	\mathcal{P}_2	\mathcal{P}_3	\mathcal{P}_4	\mathcal{P}_5	$\mathcal{N}(S)$	\mathcal{P}_1	\mathcal{P}_2	\mathcal{P}_3	\mathcal{P}_4	\mathcal{P}_5	$\mathcal{N}(M)$
mean (%)	-1.32	-1.05	-0.80	1.31	3.04	4.35	-1.14	-0.59	0.19	0.73	1.71	2.84
t-stat	-0.64	-0.50	-0.41	0.82	1.74	2.57	-0.56	-0.32	0.10	0.40	0.94	1.63
fx (%)	-1.63	-1.67	-2.71	-1.39	-0.36	1.27	-1.18	-1.14	-1.33	-2.29	-2.16	-0.97
ir (%)	0.31	0.63	1.91	2.71	3.39	3.08	0.05	0.55	1.52	3.03	3.86	3.82
net	0.11	0.07	0.01	-0.05	-0.14	-0.25	0.09	0.06	0.00	-0.04	-0.10	-0.19
Sharpe	-0.13	-0.11	-0.09	0.16	0.38	0.54	-0.11	-0.06	0.02	0.08	0.21	0.34
std (%)	10.18	9.86	9.06	8.35	8.06	8.03	10.12	9.42	8.61	9.21	8.28	8.44
skew	-0.25	-0.74	-0.55	-0.14	0.15	0.01	-0.20	-0.46	-0.35	-0.53	-0.39	-0.19
kurt	4.13	6.45	4.91	4.29	3.79	3.60	3.45	4.98	3.90	4.52	5.29	4.47
ac1	0.05	0.09	0.09	-0.01	0.08	0.04	0.04	0.02	0.06	0.00	0.21	0.10
	\mathcal{P}_1	\mathcal{P}_2	\mathcal{P}_3	\mathcal{P}_4	\mathcal{P}_5	$\mathcal{N}(L)$	\mathcal{P}_1	\mathcal{P}_2	\mathcal{P}_3	\mathcal{P}_4	\mathcal{P}_5	$\mathcal{N}(T)$
mean (%)	-0.98	-0.02	0.56	0.24	0.97	1.94	-0.74	-0.94	0.24	1.08	1.33	2.07
t-stat	-0.49	-0.01	0.28	0.14	0.53	1.15	-0.38	-0.47	0.13	0.60	0.77	1.23
fx (%)	-1.07	-0.59	-1.07	-2.50	-2.98	-1.91	-0.83	-1.42	-1.43	-1.70	-2.64	-1.81
ir (%)	0.10	0.58	1.63	2.74	3.94	3.85	0.09	0.48	1.67	2.77	3.97	3.88
net	0.07	0.04	0.00	-0.03	-0.08	-0.15	0.27	0.17	0.01	-0.14	-0.30	-0.57
Sharpe	-0.10	0.00	0.06	0.03	0.11	0.24	-0.07	-0.10	0.03	0.12	0.17	0.25
std (%)	9.86	9.29	9.05	8.80	8.59	8.22	9.96	9.53	9.17	8.95	7.89	8.18
skew	-0.21	-0.39	-0.40	-0.35	-0.54	-0.26	-0.11	-0.56	-0.56	-0.28	-0.57	-0.16
kurt	3.46	4.58	5.80	3.52	5.59	4.93	3.55	5.20	4.82	3.87	5.80	3.24
ac1	0.06	0.04	0.09	-0.04	0.15	0.10	0.03	0.06	0.02	0.00	0.19	0.06

**Table A2. Net-directional Network Portfolios and Benchmark Strategies:
Including Contemporaneous Correlations**

This table presents correlations (Panel A) and a contemporaneous regression (Panels B and C) of monthly returns of net-directional network portfolios ($\mathcal{N}(d) : d \in \{S, M, L, T\}$) on benchmark strategies — dollar (dol), carry trade (car), volatility (vol), volatility risk premium (vrp), and momentum (mom). The table reports the results for volatility linkages including contemporaneous correlations. Constants reported in the “alpha” row are expressed in percentage per annum. The numbers in rows with a grey font are t-statistics of estimates. The t-statistics are based on [Newey and West \(1987\)](#) standard errors. The last two rows report adjusted R^2 values (in percentage) and the number of observations. The sample is from January 1996 to January 2023.

Panel A: Correlations with trading strategies				
	$\mathcal{N}(S)$	$\mathcal{N}(M)$	$\mathcal{N}(L)$	$\mathcal{N}(T)$
dol	-0.36	-0.32	-0.25	-0.36
car	0.15	0.33	0.41	0.31
vol	-0.11	-0.08	-0.03	-0.15
vrp	0.25	0.29	0.27	0.27
mom	0.12	0.12	0.12	0.15
Panel B: Returns of network portfolios on benchmarks				
	$\mathcal{N}(S)$	$\mathcal{N}(M)$	$\mathcal{N}(L)$	$\mathcal{N}(T)$
alpha	3.07	0.85	-0.25	0.23
	2.09	0.56	-0.17	0.16
dollar	-0.48	-0.49	-0.43	-0.48
	-7.05	-7.03	-5.83	-6.74
car	0.15	0.32	0.38	0.33
	1.94	4.70	5.56	4.90
vol	0.11	0.05	0.02	-0.02
	1.10	0.59	0.32	-0.25
vrp	0.14	0.12	0.07	0.07
	1.79	1.51	0.92	0.99
mom	0.06	0.04	0.04	0.05
	1.15	0.71	0.64	0.93
$R^2(\%)$	23.77	33.10	35.02	34.46
Obs.	324	324	324	324

Table A3. Diversification Gains: Including Contemporaneous Correlations

This table presents the impact of adding a short-term net-directional strategy ($\mathcal{N}(S)$) to benchmark strategies — dollar (dol), carry trade (car), volatility (vol), volatility risk premium (vrp), and momentum (mom). We construct a naive 50%-50% portfolio of $\mathcal{N}(S)$ and one of the benchmark strategies. The “1/N” column presents the statistics of an equally weighted portfolio of all benchmarks and a network strategy. The table reports the results for volatility linkages including contemporaneous correlations. Mean, standard deviation, and Sharpe ratio are annualized, but the t-statistic of mean, skewness, kurtosis, and the first-order autocorrelation are based on monthly returns. The t-statistics are based on [Newey and West \(1987\)](#) standard errors. The last row in each panel shows the percentage increase in the Sharpe ratio of a diversified portfolio relative to the original benchmark strategy. The sample is from January 1996 to January 2023.

	dol	car	vol	vrp	mom	1/N
	+ $\mathcal{N}(S)$					
mean (% annual)	2.25	4.86	3.48	2.67	3.60	3.37
t-stat	2.26	3.01	2.98	1.79	2.86	3.16
Sharpe	0.50	0.66	0.59	0.39	0.56	0.70
std (%)	4.49	7.36	5.92	6.81	6.46	4.83
skew	-0.03	-0.04	0.41	0.31	0.06	0.01
kurt	3.56	3.60	4.92	5.68	3.53	3.53
ac1	0.09	0.10	-0.03	0.12	-0.01	0.09
% Δ Sharpe	2715.64	38.00	117.57	265.75	80.32	46.80

Table A4. Subsamples: Including Contemporaneous Correlations

This table presents a robustness analysis of currency strategies for subsamples from January 1996 to June 2007 and from July 2007 to January 2023. The table reports descriptive statistics of net-directional network portfolios based on volatility linkages including contemporaneous correlations. Mean, standard deviation, and Sharpe ratio are annualized, but the t-statistic of mean, skewness, kurtosis, and the first-order autocorrelation are based on monthly returns. The t-statistics are based on [Newey and West \(1987\)](#) standard errors.

	1996.1-2007.6				2007.7-2023.1			
	$\mathcal{N}(S)$	$\mathcal{N}(M)$	$\mathcal{N}(L)$	$\mathcal{N}(T)$	$\mathcal{N}(S)$	$\mathcal{N}(M)$	$\mathcal{N}(L)$	$\mathcal{N}(T)$
mean (%)	6.23	4.38	3.42	3.69	2.98	1.72	0.86	0.88
t-stat	2.14	1.31	1.06	1.22	1.53	1.00	0.52	0.48
Sharpe	0.72	0.45	0.35	0.40	0.39	0.23	0.12	0.12
std (%)	8.64	9.65	9.69	9.23	7.55	7.44	6.97	7.32
skew	-0.22	-0.39	-0.54	-0.37	0.21	0.05	0.19	0.07
kurt	2.67	4.67	4.77	2.87	4.75	3.35	3.87	3.60
ac1	0.09	0.21	0.14	0.15	-0.01	-0.04	0.03	-0.04

Table A5. Allocation Analysis for the Network Portfolios

This table presents an allocation analysis for quintile portfolios ($\mathcal{P}_i : i = 1, \dots, 5$) sorted by short-term net-directional connectedness based on volatility linkages excluding or including contemporaneous correlations. The portfolio $\mathcal{P}_1(\mathcal{P}_5)$ comprises currencies with the highest (lowest) network characteristic. The columns report the fraction of months each currency belongs to a particular portfolio. The sample is from January 1996 to January 2023.

	Excl. Contemporaneous Corr.					Incl. Contemporaneous Corr.				
	\mathcal{P}_1	\mathcal{P}_2	\mathcal{P}_3	\mathcal{P}_4	\mathcal{P}_5	\mathcal{P}_1	\mathcal{P}_2	\mathcal{P}_3	\mathcal{P}_4	\mathcal{P}_5
Australia	0.14	0.16	0.23	0.30	0.17	0.22	0.27	0.26	0.17	0.08
Brazil	0.24	0.10	0.13	0.21	0.33	0.02	0.04	0.15	0.31	0.48
Canada	0.21	0.27	0.25	0.19	0.07	0.10	0.16	0.28	0.28	0.18
Czech Republic	0.18	0.24	0.25	0.23	0.10	0.22	0.24	0.25	0.15	0.13
Denmark	0.12	0.30	0.32	0.19	0.07	0.38	0.34	0.15	0.08	0.04
Euro Area	0.17	0.31	0.33	0.14	0.04	0.53	0.33	0.10	0.04	0.01
Hungary	0.21	0.21	0.16	0.22	0.20	0.19	0.20	0.21	0.19	0.20
Japan	0.22	0.16	0.14	0.23	0.25	0.05	0.12	0.22	0.27	0.33
Mexico	0.11	0.07	0.08	0.11	0.64	0.03	0.07	0.14	0.29	0.46
New Zealand	0.13	0.23	0.24	0.28	0.11	0.13	0.21	0.32	0.22	0.12
Norway	0.13	0.27	0.35	0.19	0.06	0.51	0.27	0.13	0.07	0.02
Poland	0.17	0.17	0.15	0.20	0.31	0.20	0.24	0.22	0.20	0.15
Singapore	0.31	0.23	0.21	0.15	0.10	0.10	0.19	0.25	0.27	0.18
South Africa	0.29	0.17	0.13	0.18	0.23	0.09	0.11	0.24	0.27	0.28
South Korea	0.08	0.05	0.06	0.14	0.68	0.03	0.09	0.22	0.32	0.34
Sweden	0.16	0.31	0.35	0.15	0.03	0.44	0.33	0.16	0.05	0.02
Switzerland	0.13	0.29	0.25	0.25	0.08	0.31	0.36	0.15	0.08	0.09
Taiwan	0.46	0.17	0.09	0.14	0.14	0.02	0.08	0.23	0.28	0.39
Turkey	0.31	0.10	0.06	0.16	0.37	0.01	0.08	0.21	0.29	0.40
United Kingdom	0.22	0.16	0.18	0.25	0.19	0.15	0.19	0.23	0.21	0.22

Table A6. Equity and Hedge Fund Factors: Excluding Contemporaneous Correlations

This table presents a contemporaneous regression of monthly returns of a short-term net-directional strategy ($\mathcal{N}(S)$) on the equity and hedge fund strategies. The table reports the results for volatility linkages excluding contemporaneous correlations. For the equity factors, we consider five Fama-French factors — market (MKT), size (SMB), value (HML), profitability (RMW), investment (CMA) — and momentum (MOM), which are constructed for the U.S., developed or emerging markets. For the hedge fund factors, we consider seven Fung-Hsieh factors — bond (BOND), currency (CURR), and commodity (COMM) trend-following factors, equity market (EMKT), equity size (ESIZE), bond market (BMKT), and bond size spread (CSPREAD) factors. Constants reported in the “alpha” row are expressed in percentage per annum. The numbers in rows with a grey font are t-statistics of estimates. The t-statistics are based on [Newey and West \(1987\)](#) standard errors. The last two rows report adjusted R^2 values (in percentage) and the number of observations. The sample is from January 1996 to January 2023.

	Equity Factors			Hedge Fund Factors	
	US	Developed	Emerging		
alpha	5.44	5.79	5.20	Alpha	6.63
	3.27	3.40	2.84		3.48
MKT	-0.08	-0.10	-0.07	BOND	0.01
	-1.97	-2.36	-2.11		0.57
SMB	0.07	0.01	0.06	CURR	0.01
	1.33	0.18	0.93		0.88
HML	-0.10	-0.15	-0.02	COMM	-0.01
	-1.70	-1.75	-0.20		-0.63
RMW	0.05	0.06	0.29	EMKT	-0.11
	0.69	0.57	2.63		-2.20
CMA	0.03	0.07	0.07	ESIZE	0.03
	0.35	0.70	0.92		0.48
MOM	0.00	-0.02	-0.08	BMKT	0.01
	-0.16	-0.45	-1.69		0.92
				CSPREAD	0.01
					0.36
R^2 (%)	4.06	5.56	8.06		6.16
Obs.	324	324	324		324